

CHAPTER 14

CLIMATIC DESIGN INFORMATION

<i>Climatic Design Conditions</i>	14.1
<i>Calculating Clear-Sky Solar Radiation</i>	14.8
<i>Transposition to Receiving Surfaces of Various Orientations</i>	14.11
<i>Generating Design-Day Data</i>	14.12
<i>Estimation of Degree-Days</i>	14.13
<i>Representativeness of Data and Sources of Uncertainty</i>	14.14
<i>Other Sources of Climatic Information</i>	14.17

THIS chapter and the accompanying data summaries in PDF format provide the climatic design information for 9237 locations in the United States, Canada, and around the world. This is an increase of 1119 stations from the 2017 *ASHRAE Handbook—Fundamentals*. As in previous editions, the large number of stations made printing the whole tables impractical. Consequently, the complete table of design conditions for only an “example city” appears in this printed chapter to illustrate the table format. However, a subset of the table elements most often used is presented in the Appendix at the end of this chapter for selected stations representing major urban centers in the United States, Canada, and around the world. The complete data tables for all 9237 stations are included with both the PDF version of this chapter (downloadable from technologyportal.ashrae.org) and the Handbook Online version.

This climatic design information is commonly used for design, sizing, distribution, installation, and marketing of heating, ventilating, air-conditioning, and dehumidification equipment, as well as for other energy-related processes in residential, agricultural, commercial, and industrial applications. These summaries include values of dry-bulb, wet-bulb, and dew-point temperature, and wind speed with direction at various frequencies of occurrence. Also included are monthly degree-days to various bases, parameters to calculate clear-sky irradiance, and monthly averages of daily all-sky solar radiation. Sources of other climate information of potential interest to ASHRAE members are described later in this chapter.

Design information in this chapter was developed largely through research project RP-1847 (Roth 2021). The information includes design values of dry-bulb with mean coincident wet-bulb temperature, design wet-bulb with mean coincident dry-bulb temperature, and design dew-point with mean coincident dry-bulb temperature and corresponding humidity ratio. These data allow the designer to consider various operational peak conditions. Design values of wind speed facilitate the design of smoke management systems in buildings (Lamming and Salmon 1996, 1998).

Warm-season temperature and humidity conditions are based on annual percentiles of 0.4, 1.0, and 2.0. Cold-season conditions are based on annual percentiles of 99.6 and 99.0. The use of annual percentiles to define design conditions ensures that they represent the same probability of occurrence in any climate, regardless of the seasonal distribution of extreme temperature and humidity.

Monthly precipitation data are also included. They are used mostly to determine climate zones for ASHRAE Standard 169, but may also be helpful in developing green technologies such as vegetative roofs and stormwater harvesting.

The clear-sky solar radiation model introduced in the 2009 edition and slightly modified in the 2013 edition is unchanged in its general formulation. However, the site-specific coefficients have been recalculated, based on the latest atmospheric information available. All-sky solar radiation values are also provided; these are useful in assessing solar technologies (solar heating, photovoltaics), which are typically necessary in the quest for designing net-zero-energy buildings.

The preparation of this chapter is assigned to TC 4.2, Climatic Information.

Recent trends for a few specific elements are also listed. Although they reflect the evolution of climatic design conditions in the recent past, they are not necessarily good indicators for future trends related to climate change or other anthropogenic factors. However, they clearly make users aware of the current evolution of climate worldwide, with a general trend towards higher temperatures.

Design conditions are provided for locations for which long-term hourly observations were available (1994–2019 for most stations). Compared to the 2017 chapter, the number of U.S. stations increased from 1952 to 2220 (14% increase); Canadian stations increased from 765 to 841 (10% increase); and stations in the rest of the world increased from 5401 to 6176 (14% increase; see Figure 1 for map).

1. CLIMATIC DESIGN CONDITIONS

Table 1 shows climatic design conditions for the example city to illustrate the format of the data available as PDF downloads. The example city is a fictional station based on Atlanta, GA, over the 1990–2014 period of record; it will be used in example calculations throughout this chapter and elsewhere in the Handbook. A limited subset of these data for 1445 of the 9237 locations for 21 annual data elements is provided for convenience in the Appendix.

Station Information

The top part of the table contains station information as follows:

- Name of the observing station, state (USA) or province (Canada), country.
- World Meteorological Organization (WMO) station identifier.
- Weather Bureau Army Navy (WBAN) number (99999 denotes missing).
- Latitude of station, °N/S.
- Longitude of station, °E/W.
- Elevation of station, ft.
- Standard pressure at elevation, in psia (see Chapter 1 for equations used to calculate standard pressure).
- Time zone, h ± UTC.
- Time zone code (e.g., NAE = Eastern Time, USA and Canada). Both the PDF version of this chapter (available from technology portal.ashrae.org) and the Handbook Online version contain a list of all time zone codes used in the tables.
- Period analyzed (e.g., 94-19 = data from 1994 to 2019 were used). Note that this period does not apply to precipitation and solar radiation, which came from different data sources (see the section on Data Sources).
- Latitudes and longitudes are shown to their decimal place accuracy by default. For those stations that have had their locations visually confirmed, latitudes and longitudes are reported to four decimal places.

Annual Design Conditions

Annual climatic design conditions are contained in the first three sections following the top part of the table. They contain information as follows:

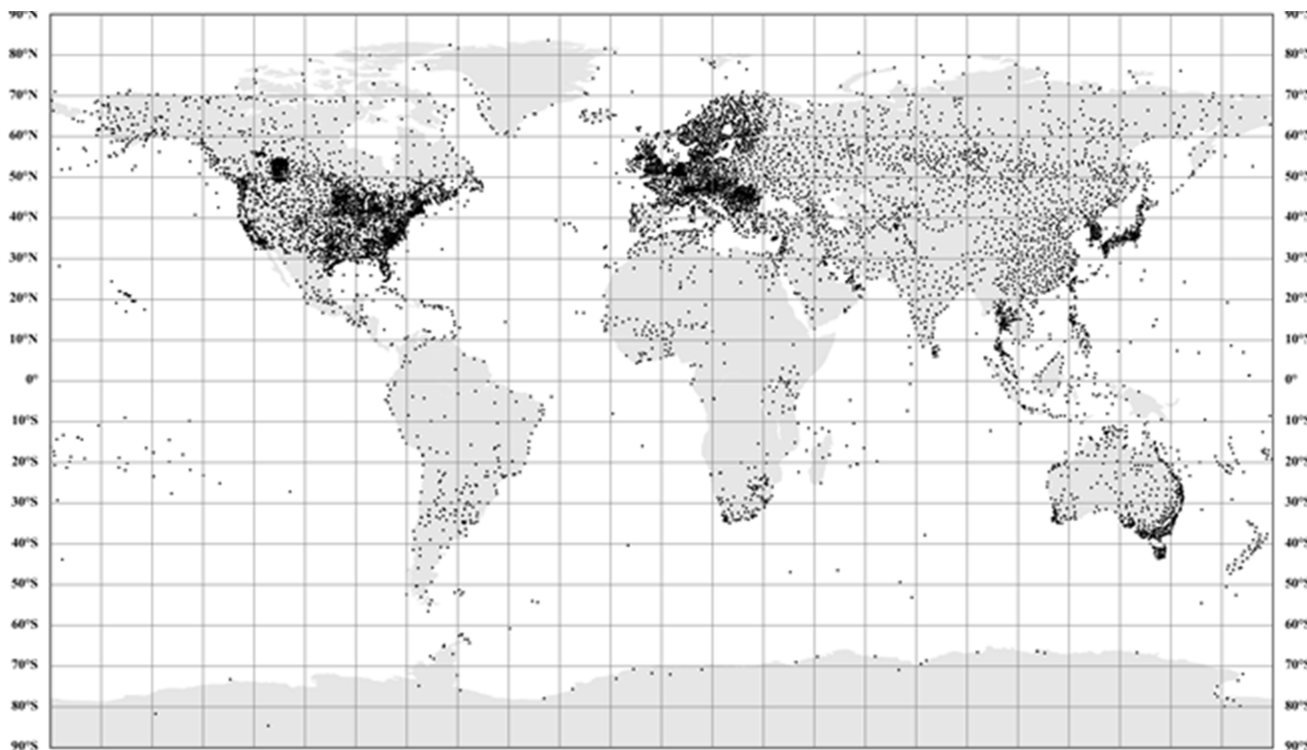


Fig. 1 Locations of Weather Stations

Annual Heating, Humidification, and Ventilation Design Conditions.

- Coldest month (i.e., month with lowest average dry-bulb temperature; 1 = January, 12 = December).
- Dry-bulb temperature corresponding to 99.6 and 99.0% annual cumulative frequency of occurrence (cold conditions), °F.
- Dew-point temperature corresponding to 99.6 and 99.0% annual cumulative frequency of occurrence, °F; corresponding humidity ratio, calculated at standard atmospheric pressure at elevation of station, grains of moisture per lb of dry air; mean coincident dry-bulb temperature, °F.
- Wind speed corresponding to 0.4 and 1.0% cumulative frequency of occurrence for coldest month, mph; mean coincident dry-bulb temperature, °F.
- Mean wind speed coincident with 99.6% dry-bulb temperature, mph; corresponding most frequent wind direction, degrees from north (east = 90°).
- Weather and shielding factor (WSF), 1/h; this factor is used in ventilation calculations as per ASHRAE Standard 62.2-2019.

Annual Cooling, Dehumidification, and Enthalpy Design Conditions.

- Hottest month (i.e., month with highest average dry-bulb temperature; 1 = January, 12 = December).
- Daily temperature range for hottest month, °F [defined as mean of the difference between daily maximum and daily minimum dry-bulb temperatures for hottest month].
- Dry-bulb temperature corresponding to 0.4, 1.0, and 2.0% annual cumulative frequency of occurrence (warm conditions), °F; mean coincident wet-bulb temperature, °F.
- Wet-bulb temperature corresponding to 0.4, 1.0, and 2.0% annual cumulative frequency of occurrence, °F; mean coincident dry-bulb temperature, °F.

- Mean wind speed coincident with 0.4% dry-bulb temperature, mph; corresponding most frequent wind direction, degrees true from north (east = 90°).
- Dew-point temperature corresponding to 0.4, 1.0, and 2.0% annual cumulative frequency of occurrence, °F; corresponding humidity ratio, calculated at the standard atmospheric pressure at elevation of station, grains of moisture per lb of dry air; mean coincident dry-bulb temperature, °F.
- Enthalpy corresponding to 0.4, 1.0, and 2.0% annual cumulative frequency of occurrence, Btu/lb; mean coincident dry-bulb temperature, °F.
- Extreme maximum wet-bulb temperature, °F.

Extreme Annual Design Conditions.

- Wind speed corresponding to 1.0, 2.5, and 5.0% annual cumulative frequency of occurrence, mph.
- Mean and standard deviation of extreme annual minimum and maximum dry-bulb temperature, °F.
- 5-, 10-, 20-, and 50-year return period values for minimum and maximum extreme dry-bulb temperature, °F.
- Mean and standard deviation of extreme annual minimum and maximum wet-bulb temperature, °F.
- 5-, 10-, 20-, and 50-year return period values for minimum and maximum extreme wet-bulb temperature, °F.

Monthly Design Conditions

Monthly design conditions are divided into subsections as follows:

Temperatures, Degree-Days, and Degree-Hours.

- Average temperature, °F (defined as the average of the high and low daily temperatures). This parameter is a prime indicator of climate and is also useful to calculate heating and cooling degree-days to any base.

- Standard deviation of average daily temperature, °F. This parameter is useful to calculate heating and cooling degree-days to any base. Its use is explained in the section on Estimation of Degree-Days.
- Heating and cooling degree-days (bases 50 and 65°F). These parameters are useful in energy estimating methods. They are also used to classify locations into climate zones in ASHRAE *Standard* 169.
- Cooling degree-hours (bases 74 and 80°F). These have historically been used in various standards, such as *Standard* 90.2-2004.

Wind.

- Monthly average wind speed, mph. This parameter is useful to estimate the wind potential at a site; however, the local topography may significantly alter this value, so close attention is needed.

Precipitation.

- Average precipitation, in. This parameter is used to calculate climate zones for *Standard* 169, and is of interest in some green building technologies (e.g., vegetative roofs, stormwater harvesting).
- Standard deviation of precipitation, in. This parameter indicates the variability of precipitation at the site.
- Minimum and maximum precipitation, in. These parameters give extremes of precipitation and are useful for green building technologies and stormwater management.

Monthly Design Dry-Bulb, Wet-Bulb, and Mean Coincident Temperatures.

These values are derived from the same analysis that results in the annual design conditions. The monthly summaries are useful when seasonal variations in solar geometry and intensity, building or facility occupancy, or building use patterns require consideration. In particular, these values can be used when determining air-conditioning loads during periods of maximum solar radiation. The values listed in the tables include

- Dry-bulb temperature corresponding to 0.4, 2.0, 5.0, and 10.0% cumulative frequency of occurrence for indicated month, °F; mean coincident wet-bulb temperature, °F.
- Wet-bulb temperature corresponding to 0.4, 2.0, 5.0, and 10.0% cumulative frequency of occurrence for indicated month, °F; mean coincident dry-bulb temperature, °F.

For a 30-day month, the 0.4, 2.0, 5.0 and 10.0% values of occurrence represent the value that occurs or is exceeded for a total of 3, 14, 36, or 72 h, respectively, per month on average over the period of record. Monthly percentile values of dry- or wet-bulb temperature may be higher or lower than the annual design conditions corresponding to the same nominal percentile, depending on the month and the seasonal distribution of the parameter at that location. Generally, for the hottest or most humid months of the year, the monthly percentile value exceeds the design condition for the same element corresponding to the same nominal percentile. For example, Table 1 shows that the annual 0.4% design dry-bulb temperature at the example city is 94.0°F; the 0.4% monthly dry-bulb temperature exceeds 94.0°F for June, July, and August, with values of 94.5, 97.6, and 97.4°F, respectively. Fifth and tenth percentiles are also provided to give a greater range in the frequency of occurrence, in particular providing less extreme options to select for design calculations.

A general, very approximate rule of thumb is that the $n\%$ annual cooling design condition is roughly equivalent to the $5n\%$ monthly cooling condition for the hottest month; that is, the 0.4% annual design dry-bulb temperature is roughly equivalent to the 2% monthly design dry-bulb temperature for the hottest month; the 1% annual value is roughly equivalent to the 5% monthly value for the

hottest month, and the 2% annual value is roughly equivalent to the 10% monthly value for the hottest month.

Mean Daily Temperature Range. These values are useful in calculating daily dry- and wet-bulb temperature profiles, as explained in the section on Generating Design-Day Data. Three kinds of profile are defined:

- Mean daily temperature range for month indicated, °F (defined as the mean difference between daily maximum and minimum dry-bulb temperatures).
- Mean daily dry- and wet-bulb temperature ranges coincident with the 5% monthly design dry-bulb temperature. This is the difference between daily maximum and minimum dry- or wet-bulb temperatures, respectively, averaged over all days where the maximum daily dry-bulb temperature exceeds the 5% monthly design dry-bulb temperature.
- Mean daily dry- and wet-bulb temperature ranges coincident with the 5% monthly design wet-bulb temperature. This is the difference between daily maximum and minimum dry- or wet-bulb temperatures, respectively, averaged over all days where the maximum daily wet-bulb temperature exceeds the 5% monthly design wet-bulb temperature.

Clear-Sky Solar Irradiance. Clear-sky irradiance parameters are useful in calculating solar-related air conditioning loads for any time of any day of the year. Parameters are provided for the 21st day of each month. The 21st of the month is usually a convenient day for solar calculations because June 21 and December 21 represent the solstices (longest and shortest days) and March 21 and September 21 are close to the equinox (days and nights have the same length). Parameters listed in the tables are

- Clear-sky optical depths for beam and diffuse irradiances, which are used to calculate beam and diffuse irradiance as explained in the section on Calculating Clear-Sky Solar Radiation.
- Clear-sky beam normal and diffuse horizontal irradiances at solar noon. These two values can be calculated from the clear-sky optical depths but are listed here for convenience.

All-Sky Solar Radiation. All-sky solar radiation parameters are useful for evaluating the potential of solar technologies (e.g., solar heating, photovoltaics), which are valuable in the design of net-zero energy buildings. Parameters listed in the tables are

- Monthly average daily global radiation on a horizontal surface. This is a traditional way to characterize the solar resource at a site.
- Standard deviation of monthly average daily radiation on a horizontal surface. This parameter gives an idea of the year-to-year variability of the solar resource at the site.

Historical Trends

Trends for annual average dry-bulb temperature, 99% dry-bulb and dew-point temperatures, 1% dry-bulb, dew-point and wet-bulb temperatures, and heating and cooling degree-days (bases 50 and 65°F) are provided. Trends are expressed in degrees Fahrenheit per decade for temperatures, and in °F-day per decade for degree-days.

The “Station only” row provides trends calculated with data from the station alone. It shows the rate (expressed per decade) at which climatic design conditions have changed. For example, a value of -0.36 in the 1% WB column indicates that yearly 1% wet-bulb temperatures have typically decreased at a rate of 0.36°F per decade over the period of record used for the calculation.

The rate of change is tested against the null hypothesis (zero trend) based on a two-sided test at the 95% level ($p \leq 0.05$). That is, a small p indicates that a zero trend is possible but very unlikely. When trends are considered statistically insignificant, or when there is insufficient data (a minimum of 15 unique years) to perform the trend analysis, the trend values simply appear as N/A.

Table 1 Design Conditions for Example City (see Table 1A for Nomenclature)

2021 ASHRAE Handbook — Fundamentals (IP)

© 2021 ASHRAE, Inc.

EXAMPLE CITY, GA, USA

WMO: 777777

Lat: 33.640N Lon: 84.430W Elev: 1027 StdP: 14.16			Time Zone: -5.00 (NAE)			Period: 90-14			WBAN: 99999								
Annual Heating, Humidification, and Ventilation Design Conditions																	
Coldest Month	Heating DB	Humidification DP/MCDB and HR						Coldest Month WS/MCDB			MCWS/PCWD to 99.6% DB						
(1) 1	21.9	26.5	9.9%	DIP	HR	MCDB	DP	HR	MCDB	WS	MCDB	WS	MCDB	MCWS	PCWD	WSF	
(a) 21.9	(b) 26.5	(c) 4.9	(d) 7.3	(e) 29.3	(f) 9.3	(g) 9.2	(h) 32.8	(i) 24.8	(j) 39.7	(k) 23.3	(l) 39.2	(m) 11.8	(n) 320	(o) 0.435	(p) (1)		
Annual Cooling, Dehumidification, and Enthalpy Design Conditions																	
Hottest Month	Hottest Month DB Range	Cooling DB/MCWB				Evaporation WB/MCDB				MCWS/PCWD to 0.4% DB							
(2) 7	16.7	94.0	74.2	91.6	73.8	89.5	73.3	77.3	88.3	76.3	86.5	75.4	84.8	8.7	300	(2)	
Dehumidification DP/MCDB and HR																	
(3) 74.3	133.3	81.3	73.4	128.9	80.3	72.6	125.5	79.6	41.3	88.3	40.3	86.7	39.5	85.4	82.4	(3)	
Extreme Annual Design Conditions																	
Extreme Annual WS			Extreme Annual Temperature						n-Year Return Period Values of Extreme Temperature								
(4) 21.3	18.9	17.0	(a) DB	(b) 15.0	(c) 96.6	(d) 4.6	(e) 3.7	(f) 11.6	(g) 99.3	(h) 8.9	(i) 101.4	(j) 6.3	(k) 103.5	(l) 3.0	(m) 106.2	(n) (4)	
(5) 12.6	79.0	4.4	WB	1.5	9.5	80.1	6.9	81.0	4.4	81.8	1.2	82.9				(5)	
Monthly Climatic Design Conditions																	
			Annual	Jan	Feb	Mar	Apr	May	Jun	Jul	Aug	Sep	Oct	Nov	Dec		
(6) DBAvg	63.0	44.5	48.0	54.9	62.6	70.5	77.3	80.1	79.5	73.9	63.6	53.5	46.4		(6)		
(7) DBStd	14.60	9.66	8.88	9.00	7.40	6.17	4.51	3.50	3.84	5.47	7.07	8.10	8.82		(7)		
(8) Temperatures, Degree-Days and Degree-Hours	653	224	132	55	6	0	0	0	0	0	4	56	176		(8)		
(9) HDD50	2640	635	477	329	127	25	1	0	0	7	111	352	576		(9)		
(10) CDD50	5391	54	76	205	385	636	819	933	914	717	425	161	66		(10)		
(11) CDD65	1901	0	1	14	56	195	370	468	449	273	67	7	1		(11)		
(12) CDH74	16445	0	3	103	435	1509	3337	4488	4173	2014	360	22	1		(12)		
(13) CDH80	6151	0	0	8	66	419	1333	1922	1726	637	40	0	0		(13)		
Wind			WSAvg	8.2	9.2	9.4	9.5	8.8	7.9	7.3	7.0	6.7	7.5	7.8	8.2	8.9	(14)
(15) PrecAvg	50.8	4.7	4.8	5.8	4.3	4.3	3.6	5.0	3.7	3.4	3.1	3.9	4.3			(15)	
(16) PrecMax	64.9	10.2	12.8	11.7	11.9	8.4	7.4	8.5	8.7	6.1	7.5	7.2	9.9			(16)	
(17) PrecMin	37.7	1.7	0.8	2.4	1.5	0.4	1.0	0.7	0.5	0.7	0.1	0.9	0.7			(17)	
(18) PrecStd	7.2	2.1	2.7	2.7	2.4	2.3	1.8	2.2	2.2	1.6	2.1	1.6	2.4			(18)	
Monthly Design Dry Bulb and Mean Coincident Wet Bulb Temperatures			DBAvg	70.5	73.4	80.8	85.0	90.2	94.5	97.6	97.4	92.8	83.5	77.4	72.3		(19)
(20) DBStd	60.8	61.3	62.6	66.5	71.3	72.9	74.8	74.3	72.0	68.3	64.1	63.1				(20)	
(21) Mean Coincident Wet Bulb Temperatures	65.7	69.1	76.9	82.0	87.0	92.0	94.1	93.7	89.0	80.9	73.3	68.6				(21)	
(22) DB	58.7	58.8	60.6	64.9	69.8	72.9	74.7	74.6	71.4	66.7	61.8	61.6				(22)	
(23) MCWB	63.0	65.9	73.5	79.2	84.6	89.8	91.6	90.9	86.4	78.2	70.3	64.6				(23)	
(24) DB	57.2	56.9	59.1	63.4	68.8	72.5	74.3	74.2	70.7	64.7	60.6	59.0				(24)	
(25) MCWB	59.5	62.7	69.8	76.1	82.1	87.4	89.1	88.3	83.8	75.3	67.1	60.9				(25)	
(26) DB	53.9	54.5	57.7	61.8	67.8	71.9	74.2	73.4	70.2	64.1	58.4	55.2				(26)	
Monthly Design Wet Bulb and Mean Coincident Dry Bulb Temperatures			WB	64.2	65.5	66.4	70.8	74.9	77.3	78.9	78.4	76.4	72.0	69.2	66.7		(27)
(27) MCDB	67.5	67.9	72.8	79.2	83.3	88.4	89.6	89.9	86.1	81.1	78.8	71.8	69.8			(28)	
(28) MCWB	61.6	62.4	64.1	68.3	72.7	75.9	77.5	77.2	74.6	70.2	66.1	63.5				(29)	
(29) DB	64.6	66.6	71.5	76.3	82.3	86.5	88.3	88.4	83.2	75.9	70.0	66.4				(30)	
(30) MCDB	58.6	59.5	62.1	66.4	71.3	74.9	76.5	76.2	73.5	68.7	63.5	60.3				(31)	
(31) DB	61.9	64.0	70.0	74.4	80.6	85.0	86.7	86.1	80.9	73.8	67.7	64.1				(32)	
(32) MCDB	55.2	56.3	60.0	64.5	69.9	73.8	75.4	75.2	72.6	66.9	60.5	56.3				(33)	
(33) DB	58.3	60.6	67.0	72.3	78.6	83.1	84.9	84.2	79.5	72.3	65.4	59.8				(34)	
Mean Daily Temperature Range			MDBR	17.3	18.2	19.2	19.8	18.2	17.2	16.7	16.4	16.5	18.1	18.7	16.6		(35)
(35) 5% DB	19.5	20.9	22.5	22.0	20.1	20.2	19.5	19.1	20.4	20.9	19.5					(36)	
(36) 5% MCWB	13.6	13.3	11.0	9.5	7.5	6.6	6.1	6.0	6.8	8.9	11.7	13.2				(37)	
(37) 5% MCDB	16.0	17.5	17.9	18.2	17.3	17.3	17.5	16.8	15.3	14.9	16.8	16.8				(38)	
(38) 5% WB	13.2	13.8	11.0	9.8	7.7	6.9	6.4	6.1	6.9	8.9	12.9	13.6				(39)	
Clear-Sky Solar Irradiance			taub	0.310	0.315	0.347	0.386	0.440	0.473	0.515	0.515	0.417	0.363	0.333	0.311		(40)
(40) taud	2.538	2.521	2.453	2.324	2.213	2.168	2.066	2.052	2.312	2.460	2.484	2.554				(41)	
(41) Etb at Noon	288	298	295	286	270	260	249	246	268	277	276	281				(42)	
(42) Edt at Noon	26	29	34	40	46	48	53	52	39	31	27	24				(43)	
All-Sky Solar Radiation			RadAvg	852	1054	1407	1751	1904	1954	1858	1726	1496	1275	963	738		(44)
(44) RadStd	50	122	109	126	164	162	134	103	148	163	82	73				(45)	
Historical Trends																	
			DBAvg	99% DB	99% DP	1% DB	1% WB	1% DP	HDD50	HDD65	CDD50	CDD65					
(46) Station Only	N/A	N/A	N/A	N/A	-0.36	-0.41	N/A	N/A	N/A	N/A	N/A					(46)	
(47) Regional (1 neighbor)	N/A	N/A	N/A	N/A	-0.43	-0.47	N/A	N/A	N/A	N/A	N/A					(47)	

Nomenclature: See separate page.

Table 1A Nomenclature for Tables of Climatic Design Conditions

CDD _n	Cooling degree-days base n°F, °F-day
CDH _n	Cooling degree-hours base n°F, °F-hour
DB	Dry-bulb temperature, °F
DBAvg	Average daily dry-bulb temperature, °F
DBSD	Standard deviation of average daily dry-bulb temperature, °F
DP	Dew-point temperature, °F
Ebn,noon	Clear-sky beam normal irradiances at solar noon, Btu/h·ft ²
Edh,noon	Clear-sky diffuse horizontal irradiance at solar noon, Btu/h·ft ²
Elev	Elevation, ft
Enth	Enthalpy, Btu/lb base 0°F and 1 atm pressure
HDD _n	Heating degree-days base n°F, °F-day
HR	Humidity ratio, gr _{moisture} /lb _{dry air}
Lat	Latitude, °N
Long	Longitude, °E
MCDB	Mean coincident dry-bulb temperature, °F
MCDBR	Mean coincident dry-bulb temperature range, °F
MCWB	Mean coincident wet-bulb temperature, °F
MCWBR	Mean coincident wet-bulb temperature range, °F
MCWS	Mean coincident wind speed, mph
MDBR	Mean dry-bulb temperature range, °F
PCWD	Pervailing coincident wind direction, ° (0 = North; 90 = East)
Period	Years used to calculate the design conditions
PrecAvg	Average precipitation, in.
PrecMax	Maximum precipitation, in.
PrecMin	Minimum precipitation, in.
PrecStd	Standard deviation of precipitation, in.
RadAvg	Monthly mean daily all-sky radiation, Btu/ft ² ·day
RadStd	Standard deviation of monthly mean daily radiation, Btu/ft ² ·day
StdP	Standard pressure at station elevation, psi
taub	Clear-sky optical depth for beam irradiance
taud	Clear-sky optical depth for diffuse irradiance
Time Zone	Hours ahead or behind UTC, and time zone code
WB	Wet-bulb temperature, °F
WBAN	Weather Bureau Army Navy number
WMO#	Station identifier from the World Meteorological Organization
WS	Wind speed, mph
WSAvg	Monthly average wind speed, mph
WSF	Weather and shielding factor, 1/h

Note: Numbers (1) to (47) and letters (a) to (p) are row and column references to quickly point to an element in the table. For example, the 5% design wet-bulb temperature for July can be found in row (31), column (k).

Trends are often hard to detect for individual stations. Grouping stations together may provide a stronger signal and make it easier to identify a significant trend. The “Regional” trend evaluates data from all stations within 125 mi of the station of interest and may provide better confidence for some trends. Note that depending on station density, there may be upwards of 100 neighbors or few if any stations. For those stations with no neighbors the regional trend data will appear as N/A.

How to use the trend estimates is left to individual practitioners, as there is at this stage no accepted method of designing for future climate. The trends reported here, or indeed the lack thereof, reflect only what has occurred over the period of record utilized for the station. A significant trend can result from undocumented location changes, equipment replacement or error (e.g., sensor “drift”), nearby topographic modifications (trees, buildings), and, finally,

larger scale (local, synoptic, global) changes in climate. Past trends are not necessarily indicators of future trends, and the trends reported here are based on a shorter period of record than used for climate change research, which generally consider periods of 30 to over 100 years. The section on Effects of Climate Change later in this chapter gives further consideration to this topic, while Chapter 36 of this volume provides an overview of climate science together with a discussion of climate change mitigation and adaption.

Data Sources

The following primary sources of observational data sets were used in calculating design values:

- Most stations were sourced through the Integrated Surface Database (ISD) from NOAA (www.ncdc.noaa.gov) (Smith et al. 2011) for the years 1982–2019.
- For most Canadian stations, meteorological data were obtained directly from Environment and Climate Change Canada (climate.weather.gc.ca) for the years 1982–2019. A few stations with inadequate data were sourced from the ISD.

In most cases, the period used in the calculations spanned 26 years (1994 to 2019). This choice of period is a compromise between trying to derive design conditions from the longest possible period, and using the most recent data to capture climatic or land-use trends from the past two decades. The actual number of years used in the calculations for a given station depends on the amount of missing data, and, as discussed in the next section, may be as little as 8 years. The first and last years of the period used to calculate design conditions are listed in the top section of the tables of climatic design conditions, as shown in Table 1 for the example city. For a limited number of stations, periods extending as far back as 1982 to 2019 were used instead of 1994 to 2019 because that time frame lacked the necessary data.

Precipitation data were derived from a number of sources, including station observational data from the Global Historical Climatology Network, version 2 (GHCN 2015), as well as gridded data from the Global Precipitation Climatology Centre, Full Data Monthly Product Version 2018 (GPCC 2018; resolution is 0.25°×0.25°, 0.5°×0.5°, and 1.0°×1.0°), and the Global Precipitation Climate Project, Version 2.3 Combined Precipitation Data Set (GPCP 2020; resolution is 2.5°×2.5°). These sources are based on different periods: 1960 to 2019 for GHCN, 1990 to 2016 for GPCC and 1990 to 2019 for GPCP.

Clear-sky solar irradiance parameters listed in the tables constitute a simple parameterization of the more sophisticated REST2 broadband clear-sky radiation model (Gueymard 2008; Gueymard and Thevenard 2009; Thevenard 2009). The REST2 model requires detailed knowledge of various atmospheric constituents, such as aerosols, water vapor, or ozone. To extend applicability of the model to the whole world, multiple data sets, mainly derived from space observations and reanalysis models, were used to obtain these inputs. These sources of data have not changed since the 2017 edition, so there should be few changes in site-specific coefficients. Water vapor, ozone, and ground albedo data are derived from the National Aeronautics and Space Administration (NASA) Modern-Era Retrospective Analysis for Research and Applications, version 2 (MERRA-2) reanalysis dataset (Molod et al. 2015), corrected for elevation in the case of water vapor (Gueymard and Thevenard 2009). The period of data is uniform, from 2000 to 2014. An exception is nitrogen dioxide, for which a database from Ozone Monitoring Instrument (OMI) satellite observations (aura.gsfc.nasa.gov/omi.html) is used over the period 2005 to 2014. Pressure is estimated from station’s elevation.

Aerosol turbidity data (in the form of separate evaluations of aerosol optical depth and Ångström exponent) received special

attention, because they are the primary inputs that affect the accuracy of direct and diffuse irradiance predictions under clear skies. Spaceborne retrievals of aerosol optical depth at various wavelengths from NASA's Multi-angle Imaging SpectroRadiometer (MISR; www-misr.jpl.nasa.gov) and two Moderate Resolution Imaging Spectroradiometer (MODIS; modis-atmos.gsfc.nasa.gov) instruments were used between 2000 and 2014 and compared to reference data from a large number of ground-based sites, mostly from the Aerosol Robotic Network (AERONET; aeronet.gsfc.nasa.gov), after appropriate scale-height corrections to remove artifacts from the effect of elevation (Guemard and Thevenard 2009). Regional corrections of the satellite data were devised to remove as much bias as possible, compared to the reference ground-based data. To fill missing data or correct biased satellite observations, modeled aerosol datasets were used, including 10 years (2003 to 2012) of simulated monthly-average aerosol optical depth from the Monitoring Atmospheric Composition and Climate (MACC) reanalysis model (Eskes et al. 2015; Inness et al. 2013) and 13 years (2002 to 2014) of MERRA-2 reanalysis data (Molod et al. 2015). Results from the REST2 model (Guemard 2008) were then fitted to the simple two-parameter model described in this chapter. The fits enable a concise formulation requiring tabulation, on a monthly basis, of only two parameters per station, referred to here as the clear-sky beam and diffuse optical depths. Details about the fitting procedure can be found in Thevenard and Guemard (2013).

Global horizontal irradiance at the surface, and its standard deviation, were calculated from the Clouds and the Earth's Radiant Energy System (CERES) Energy Balanced and Filled (EBAF) dataset (ceres.larc.nasa.gov). From the available $1^\circ \times 1^\circ$ dataset, a bilinear interpolation, without altitude adjustment, was made given the station latitude and longitude for the period 2000 to 2018.

Calculation of Design Conditions

Values of ambient dry-bulb, dew-point, and wet-bulb temperature and wind speed corresponding to the various annual percentiles represent the value that is exceeded on average by the indicated percentage of the total number of hours in a year (8760). The 0.4, 1.0, 2.0, and 5.0% values are exceeded on average 35, 88, 175, and 438 h per year, respectively, for the period analyzed. The design values occur more frequently than the corresponding nominal percentile in some years and less frequently in others. The 99.0 and 99.6% (cold-season) values are defined in the same way but are usually viewed as the values for which the corresponding weather element is less than the design condition for 88 and 35 h, respectively.

Simple design conditions were obtained by binning hourly data into frequency tables, then deriving from the binned data the design condition having the probability of being exceeded a certain percentage of the time. Mean coincident values were obtained by double-binning the hourly data into joint frequency matrices, then calculating the mean coincident value corresponding to the simple design condition.

Coincident temperature ranges were also obtained by double-binning daily temperature ranges (daily maximum minus minimum) versus maximum daily temperature. The mean coincident daily range was then calculated by averaging all bins above the simple design condition of interest.

The weather data sets used for the calculations often contain missing values (either isolated records, or because some stations report data only every third hour). Gaps up to 6 h were filled by linear interpolation to provide as complete a time series as possible. Dry-bulb temperature, dew-point temperature, station pressure, and humidity ratio were interpolated. However, wind speed and direction were not interpolated because of their more stochastic and unpredictable nature.

Some stations in the ISD data set also provide data that were not recorded at the beginning of the hour. When data at the exact hour

were missing, they were replaced by data up to 0.5 h before or after, when available.

Finally, psychrometric quantities such as wet-bulb temperature or enthalpy are not contained in the weather data sets. They were calculated from dry-bulb temperature, dew-point temperature, and station pressure using the psychrometric equations in Chapter 1.

Measures were taken to ensure that the number and distribution of missing data, both by month and by hour of the day, did not introduce significant biases into the analysis. Annual cumulative frequency distributions were constructed from the relative frequency distributions compiled for each month. Each individual month's data were included if they met the following screening criteria for completeness and unbiased distribution of missing data after data filling:

- The number of hourly dry-bulb temperature values for the month, after filling by interpolation, had to be at least 85% of the total hours for the month.
- The difference between the number of day and nighttime dry-bulb temperature observations had to be less than 60.

Although the nominal period of record selected for this analysis was 26 years (1994 to 2019 for most stations), some variation and gaps in observed data meant that some months' data were unusable because of incompleteness. Some months were also eliminated during additional quality control checks. A station's dry-bulb temperature design conditions were calculated only if there were data from at least 8 months that met the quality control and screening criteria from the period analyzed for each month of the year. For example, there had to be 8 months each of January, February, March, etc. for which data met the completeness screening criteria. These criteria were ascertained from results of RP-1171 (Hubbard et al. 2004) and were the same as used in calculating the design conditions in the 2001 to 2017 editions of the *ASHRAE Handbook—Fundamentals*.

Dew-point temperature, wet-bulb temperature, and enthalpy design conditions were calculated for a given month only if the number of dew-point, wet-bulb, or enthalpy values was greater than 85% of the minimum number of dry-bulb temperature values defined previously; wind speed and direction conditions were calculated for a given month only if the number of values was greater than 28.3% (i.e., one-third of 85%) the minimum number of dry-bulb temperature values. For example, a month of January was included in calculations if the number of dry-bulb temperature values exceeded 85% of 744 h, or 633 h. The month was included in calculation of dew-point temperature design conditions only if dew-point temperature was present for at least 85% of 633 h, or 538 h. The month was included in calculation of wind speed design conditions only if wind speed was present for at least 28.3% of 633 h, or 179 h.

Annual dry-bulb temperature extremes were calculated only for years that were 85% complete. At least 8 annual extremes were required to calculate the mean and standard deviation of extreme annual dry-bulb temperatures.

Daily minimum and maximum temperatures were calculated only for complete days; so were daily temperature ranges and mean coincident temperature ranges.

The weather and shielding factor is calculated using the entire period of record by first calculating the hourly weather-induced infiltration for a baseline building as per Chapter 16 and then converting this time series into a single effective infiltration dimensionless number using the methodology of Turner et al. (2012).

Trends were calculated only for stations having at least 15 distinct full years of data.

Details about quality checks and other steps taken during data processing to ensure results as free from error as possible are detailed in Roth (2017, 2021).

Differences from Previously Published Design Conditions

- Climatic design conditions in this chapter are generally similar to those in previous editions, because similar if not identical analysis procedures were used. There are some differences, however, owing to a more recent period of analysis (generally 1994–2019 versus 1990–2014 for the 2017 edition). For example, when compared to the 2017 edition, 99.6% heating dry-bulb temperatures have increased by 0.22°F on average, and 0.4% cooling dry-bulb temperatures have increased by 0.25°F on average. Similar trends are observed for other design temperatures. The root mean square differences are 0.89°F for the 99.6% heating dry-bulb values and 0.58°F for 0.4% cooling dry-bulb. The increases noted here are generally consistent with the discussion in the section on Effects of Climate Change.
- Further details concerning differences between design conditions in the 2017, 2013, 2009, 2005, and 2001 editions are described respectively in Roth (2016), Thevenard and Gueymard (2013), Thevenard (2009), and Thevenard et al. (2005). Differences between the 1993 and previous editions are described in Colliver et al. (2000).

Applicability and Characteristics of Design Conditions

Climatic design values in this chapter represent different psychrometric conditions. Design data based on dry-bulb temperature represent peak occurrences of the sensible component of ambient outdoor conditions. Design values based on wet-bulb temperature are related to the enthalpy of the outdoor air. Conditions based on dew point relate to the peaks of the humidity ratio. The designer, engineer, or other user must decide which set(s) of conditions and probability of occurrence apply to the design situation under consideration. Additional sources of information on frequency and duration of extremes of temperature and humidity are provided in the section on Other Sources of Climatic Information. Further information is available from Harriman et al. (1999). This section discusses the intended use of design conditions in the order they appear in Table 1.

Annual Heating, Humidification, and Ventilation Design Conditions. The month with the lowest mean dry-bulb temperature is used, for example, to determine the time of year where the maximum heating load occurs.

The 99.6 and 99.0% design conditions are often used in sizing heating equipment.

The humidification dew-point and mean coincident dry-bulb temperatures and humidity ratio provide information for cold-season humidification applications.

Wind design data provide information for estimating peak loads accounting for infiltration: extreme wind speeds for the coldest month, with the mean coincident dry-bulb temperature; and mean wind speed and direction coincident to the 99.6% design dry-bulb temperature.

The weather and shielding factor (WSF) is used in ASHRAE Standard 62.2-2019 to calculate the effective annual average infiltration rate, in order to determine ventilation rates in buildings.

Annual Cooling, Dehumidification, and Enthalpy Design Conditions. The month with the highest mean dry-bulb temperature is used, for example, to determine the time of year where the maximum sensible cooling load occurs, not taking into account solar loads.

The mean daily dry-bulb temperature range for the hottest month is the mean difference between the daily maximum and minimum temperatures during the hottest month and is calculated from the extremes of the hourly temperature observations. The true maximum and minimum temperatures for any day generally occur between hourly readings. Thus, the mean maximum and minimum temperatures calculated in this way are about 1°F less extreme than the mean daily extreme temperatures observed with maximum and

minimum thermometers. This results in the true daily temperature range generally about 2°F greater than that calculated from hourly data. The mean daily dry-bulb temperature range is used in cooling load calculations.

The 0.4, 1.0, and 2.0% dry-bulb temperatures and mean coincident wet-bulb temperatures often represent conditions on hot, mostly sunny days. These are often used in sizing cooling equipment such as chillers or air-conditioning units.

Design conditions based on wet-bulb temperature represent extremes of the total sensible plus latent heat of outdoor air. This information is useful for design of cooling towers, evaporative coolers, and outdoor-air ventilation systems.

The mean wind speed and direction coincident with the 0.4% design dry-bulb temperature is used for estimating peak loads accounting for infiltration.

Design conditions based on dew-point temperatures are directly related to extremes of humidity ratio, which represent peak moisture loads from the weather. Extreme dew-point conditions may occur on days with moderate dry-bulb temperatures, resulting in high relative humidity. These values are especially useful for humidity control applications, such as desiccant cooling and dehumidification, cooling-based dehumidification, and outdoor-air ventilation systems. The values are also used as a check point when analyzing the behavior of cooling systems at part-load conditions, particularly when such systems are used for humidity control as a secondary function. Humidity ratio values are calculated from the corresponding dew-point temperature and the standard pressure at the location's elevation.

Annual enthalpy design conditions give the annual enthalpy for the cooling season; this is used for calculating cooling loads caused by infiltration and/or ventilation into buildings. Enthalpy represents the total heat content of air (the sum of its sensible and latent energies). Cooling loads can be calculated knowing the conditions of both the outdoor ambient and the building's interior air.

The extreme maximum wet-bulb temperature provides the highest wet-bulb temperature observed over the entire period of analysis and is the most extreme condition observed during the data record for evaporative processes such as cooling towers. For most locations, the extreme maximum wet-bulb value is significantly higher than the 0.4% wet-bulb (discussed previously) and should be used only for design of critical applications where an occasional short-duration capacity shortfall is not acceptable.

Extreme Annual Design Conditions. Extreme annual design wind speeds are used in designing smoke management systems.

The mean and standard deviation of the extreme annual maximum and minimum dry-bulb temperatures are used to calculate the probability of occurrence of very extreme conditions. These can be required for design of equipment to ensure continuous operation and serviceability regardless of whether the heating or cooling loads are being met. These values were calculated from extremes of hourly temperature observations. The true maximum and minimum temperatures for any day generally occur between hourly readings. Thus, the mean maximum and minimum temperatures calculated in this way are generally about 1°F less extreme than the mean daily extreme temperatures observed with maximum and minimum thermometers.

The 5-, 10-, 20- and 50-year return periods for maximum and minimum extreme dry-bulb temperature are also listed in the table. Return period (or recurrence interval) is defined as the reciprocal of the annual probability of occurrence. For instance, the 50-year return period maximum dry-bulb temperature has a probability of occurring or being exceeded of 2.0% (i.e., 1/50) each year. This statistic does not indicate how often the condition will occur in terms of the number of hours each year (as in the design conditions based on percentiles) but describes the probability of the condition occurring at all in any year. The following method can be used to estimate the return period (recurrence interval) of extreme temperatures:

$$T_n = M + IFs \quad (1)$$

where

T_n = n -year return period value of extreme dry-bulb temperature to be estimated, years

M = mean of annual extreme maximum or minimum dry-bulb temperatures, °F

s = standard deviation of annual extreme maximum or minimum dry-bulb temperatures, °F

I = 1 if maximum dry-bulb temperatures are being considered
= -1 if minimum dry-bulb temperatures are being considered

$$F = -\frac{\sqrt{6}}{\pi} \left\{ \gamma + \ln \left[\ln \left(\frac{n}{n-1} \right) \right] \right\}, \text{ where } \gamma \text{ is Euler's number or } 0.5772\dots$$

For example, the 50-year return period extreme maximum dry-bulb temperature estimated for the example city is 106.2°F (according to Table 1, $M = 96.6$ °F, $s = 3.7$, and $n = 50$; $I = 1$). Similarly, the 50-year return period extreme minimum dry-bulb temperature for the example city is 3.0°F [$M = 15.0$ °F, $s = 4.6$, and $n = 50$; $I = -1$]. The n -year return periods can be obtained for most stations using ASHRAE's Weather Data Viewer, which is discussed in the section on Other Sources of Climatic Information.

Similarly, this section lists the parameters required to calculate the 5-, 10-, 20- and 50-year return periods for maximum and minimum extreme wet-bulb temperature. The maximum conditions in particular may be useful in determining very extreme wet-bulb temperatures during which evaporative systems may have to operate. Also, wet-bulb temperatures exceeding 95°F are known to impede the ability of humans to effectively shed heat through sweat evaporation.

Calculation of the n -year return period is based on assumptions that annual maxima and minima are distributed according to the Gumbel (Type 1 Extreme Value) distribution and are fitted with the method of moments (Lowery and Nash 1970). The uncertainty or standard error using this method increases with standard deviation, value of return period, and decreasing length of the period of record. It can be significant. For instance, the standard error in the 50-year return period maximum dry-bulb temperature estimated at a location with a 12-year period of record can be 5°F or more. Thus, the uncertainties of return period values estimated in this way are greater for stations with fewer years of data than for stations with the complete period of record from 1994 to 2019.

Temperatures, Degree-Days, and Degree-Hours. Monthly average temperatures and standard deviation of daily average temperatures are calculated using the averages of the minimum and maximum temperatures for each complete day within the period analyzed. They are used to estimate heating and cooling degree-days to any base, as explained in the section on Estimation of Degree-Days.

Heating and cooling degree-days (base 50 or 65°F) are calculated as the sum of the differences between daily average temperatures (calculated as the average of the daily minimum and maximum temperatures) and the base temperature. For example, the number of **heating degree-days (HDD)** in the month is calculated as

$$HDD = \sum_{i=1}^N (T_{base} - \bar{T}_i)^+ \quad (2)$$

where N is the number of days in the month, T_{base} is the reference temperature to which the degree-days are calculated, and \bar{T}_i is the mean daily temperature calculated by adding the maximum and minimum temperatures for the day, then dividing by 2. The $+$ superscript indicates that only positive values of the bracketed quantity are taken into account in the sum. Similarly, monthly **cooling degree-days (CDD)** are calculated as

$$CDD = \sum_{i=1}^N (\bar{T}_i - T_{base})^+ \quad (3)$$

Degree-days are used in energy estimating methods, and to classify stations into climate zones for ASHRAE Standard 169.

Degree-hours are calculated in a similar way but using hourly temperatures instead of daily temperatures. They are also used in energy estimating methods. However, their higher temporal resolution does not necessarily translate to better correlation with building loads because of building thermal lag.

Monthly Design Dry-Bulb and Mean Coincident Wet-Bulb Temperatures. These values provide design conditions for processes driven by dry-bulb air temperature. In particular, air-conditioning cooling loads are generally based on dry-bulb design conditions (plus clear-sky solar irradiance).

Monthly Design Wet-Bulb and Mean Coincident Dry-Bulb Temperatures. Wet-bulb design conditions are of use in analysis of evaporative coolers, cooling towers, and other equipment involving evaporative transfer. Note also that air wet-bulb temperature and enthalpy are closely related, so applications with large ventilation flow rates may have maximum cooling requirements under high wet-bulb conditions.

Mean Daily Temperature Range. Mean daily range values are computed using all days of the month, as opposed to coincident values that derive from design days. Mean daily range values have been published in previous Handbook editions and are included for completeness. Coincident daily range values should be used for generating design-day profiles.

Clear-Sky Solar Irradiance. Clear-sky solar irradiance data are used in load calculation methods. **Beam normal irradiance** refers to solar radiation emanating directly from the solar disk and measured perpendicularly to the rays of the sun. **Diffuse horizontal irradiance** refers to solar radiation emanating from the sky dome, sun excluded, and measured on a horizontal surface. Because the beam and diffuse irradiances vary during the course of the day, current load calculation methods require their estimation at various times, which can be done with the method described in the section on Calculating Clear-Sky Solar Radiation. The method uses the clear-sky optical depths τ_b and τ_d , listed in Table 1 as $taub$ and $taud$, respectively, as inputs. Clear-sky beam normal and diffuse horizontal irradiances at solar noon are also listed in Table 1 for convenience.

All-Sky Solar Radiation. All-sky solar radiation data are used in the design of solar energy systems (either thermal or photovoltaic). **Monthly average daily radiation on the horizontal** refers to average amount of solar radiation received on a horizontal surface during the course of a day, for the month under consideration. The **standard deviation of monthly average daily radiation on the horizontal** is the standard deviation of the previous monthly quantity, calculated over the period of analysis used for the Handbook, and is an indicator of the year-to-year variability of solar radiation.

2. CALCULATING CLEAR-SKY SOLAR RADIATION

Knowledge of clear-sky solar radiation at various times of year and day is required by several calculation methods for heat gains in HVAC loads and solar energy applications. The tables of climatic design conditions include the parameters required to calculate clear-sky beam and diffuse solar irradiances using the equations in the following section. The section on Transposition to Receiving Surfaces of Various Orientations explains how to use these values to calculate clear-sky solar radiation incident on arbitrary surfaces.

Note that in all equations in this section, *angles are expressed in degrees*. This includes the arguments appearing in trigonometric functions.

Table 2 Approximate Astronomical Data for 21st Day of Each Month

Month	Jan	Feb	Mar	Apr	May	Jun	Jul	Aug	Sep	Oct	Nov	Dec
Day of year	21	52	80	111	141	172	202	233	264	294	325	355
E_o , Btu/h·ft ²	447	443	437	429	423	419	420	424	430	437	444	447
Equation of time (ET), min	-10.6	-14.0	-7.9	1.2	3.7	-1.3	-6.4	-3.6	6.9	15.5	13.8	2.2
Declination δ , degrees	-20.1	-11.2	-0.4	11.6	20.1	23.4	20.4	11.8	-0.2	-11.8	-20.4	-23.4

Table 3 Time Zones in United States and Canada

Time Zone Name	TZ (Hours ± UTC)	Local Standard Meridian Longitude (°E)
Newfoundland standard time	-3.5	-52.5
Atlantic standard time	-4	-60
Eastern standard time	-5	-75
Central standard time	-6	-90
Mountain standard time	-7	-105
Pacific standard time	-8	-120
Alaska standard time	-9	-135
Hawaii-Aleutian standard time	-10	-150

Solar Constant and Extraterrestrial Solar Radiation

The **solar constant** E_{sc} is defined as the intensity of solar radiation on a surface normal to the sun's rays, just beyond the earth's atmosphere, at the average earth-sun distance. One frequently used value is that proposed by the World Meteorological Organization in 1981, $E_{sc} = 433.3 \text{ Btu/h}\cdot\text{ft}^2$ (Iqbal 1983).

Because the earth's orbit is slightly elliptical, the **extraterrestrial radiant flux** E_o varies throughout the year, reaching a maximum of 447.6 Btu/h·ft² near the beginning of January, when the earth is closest to the sun (aphelion) and a minimum of 419.1 Btu/h·ft² near the beginning of July, when the earth is farthest from the sun (perihelion). Extraterrestrial solar irradiance incident on a surface normal to the sun's ray can be approximated with the following equation:

$$E_o = E_{sc} \left\{ 1 + 0.033 \cos \left[360^\circ \frac{(n - 3)}{365} \right] \right\} \quad (4)$$

where n is the day of year (1 for January 1, 32 for February 1, etc.) and the argument inside the cosine is in degrees. Table 2 tabulates values of E_o for the 21st day of each month.

Equation of Time and Solar Time

The earth's orbital velocity also varies throughout the year, so **apparent solar time (AST)**, as determined by a solar time sundial, varies somewhat from the **mean time** kept by a clock running at a uniform rate. This variation is called the **equation of time (ET)** and is approximated by the following formula (Iqbal 1983):

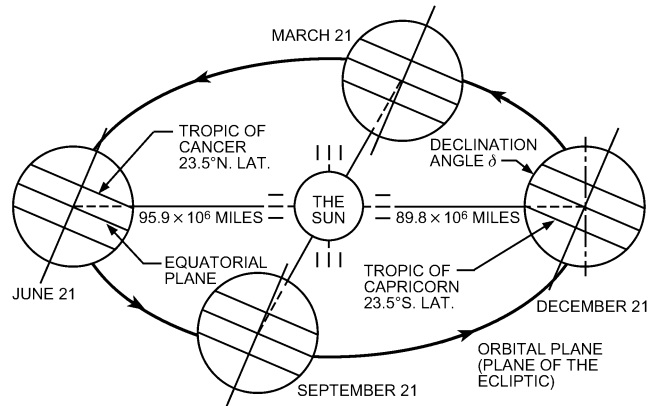
$$\begin{aligned} ET = & 2.2918[0.0075 + 0.1868 \cos(\Gamma) - 3.2077 \sin(\Gamma) \\ & - 1.4615 \cos(2\Gamma) - 4.089 \sin(2\Gamma)] \end{aligned} \quad (5)$$

with ET expressed in minutes and

$$\Gamma = 360^\circ \frac{n - 1}{365} \quad (6)$$

Table 2 tabulates the values of ET for the 21st day of each month.

The conversion between local standard time and solar time involves two steps: the equation of time is added to the local standard time, and then a longitude correction is added. This longitude correction is four minutes of time per degree difference between the **local (site) longitude** and the longitude of the **local standard meridian (LSM)** for that time zone; hence, AST is related to the **local standard time (LST)** as follows:

**Fig. 2 Motion of Earth around Sun**

$$AST = LST + ET/60 + (LON - LSM)/15 \quad (7)$$

where

AST = apparent solar time, decimal hours

LST = local standard time, decimal hours

ET = equation of time in minutes, from Table 2 or Equation (5)

LSM = longitude of local standard time meridian, °E of Greenwich (negative in western hemisphere)

LON = longitude of site, °E of Greenwich

Most standard meridians are found every 15° from 0° at Greenwich, U.K., with a few exceptions, such as the province of Newfoundland in Canada. Standard meridian longitude is related to time zone as follows:

$$LSM = 15TZ \quad (8)$$

where TZ is the time zone, expressed in hours ahead or behind **coordinated universal time (UTC)**. TZ is listed for each station in both the PDF version of this chapter (available from technologyportal.ashrae.org) and the Handbook Online version. Table 3 lists time zones and standard time meridians for the United States and Canada.

If **daylight saving time (DST)** is to be used, rather than local standard time, an additional correction has to be performed. In most locales, local standard time can be obtained from daylight savings time by subtracting one hour:

$$LST = DST - 1 \quad (9)$$

where DST is in decimal hours.

Declination

Because the earth's equatorial plane is tilted at an angle of 23.45° to the orbital plane, the **solar declination** δ (the angle between the earth/sun line and the equatorial plane) varies throughout the year, as shown in Figure 2. This variation causes the changing seasons with their unequal periods of daylight and darkness. Declination can be obtained from astronomical or nautical almanacs; however, for most engineering applications, the following equation provides sufficient accuracy:

$$\delta = 23.45 \sin\left(360^\circ \frac{n + 284}{365}\right) \quad (10)$$

where δ is in degrees and the argument inside the sine is also in degrees. Table 2 provides δ for the 21st day of each month.

Sun Position

The sun's position in the sky is conveniently expressed in terms of the solar altitude above the horizontal and the solar azimuth measured from the south (Figure 3). The solar altitude angle β is defined as the angle between the horizontal plane and a line emanating from the sun. Its value ranges from 0° when the sun is on the horizon, to 90° if the sun is directly overhead. Negative values correspond to night times. The solar azimuth angle ϕ is defined as angular displacement from south of the projection, on the horizontal plane, of the earth/sun line. By convention, it is counted positive for afternoon hours and negative for morning hours.

Solar altitude and azimuth angles, in turn, depend on the local latitude L ($^\circ$ N, negative in the southern hemisphere), the solar declination δ , which is a function of the date [see Table 2 or Equation (10)]; and the hour angle H , defined as the angular displacement of the sun east or west of the local meridian caused by the rotation of the earth, and expressed in degrees as

$$H = 15(\text{AST} - 12) \quad (11)$$

where AST is the apparent solar time [Equation (7)]. H is zero at solar noon, positive in the afternoon, and negative in the morning.

Equation (12) relates the solar altitude angle β to L , δ , and H :

$$\sin \beta = \cos L \cos \delta \cos H + \sin L \sin \delta \quad (12)$$

Note that at solar noon, $H = 0$ and the sun reaches its maximum altitude in the sky:

$$\beta_{\max} = 90^\circ - |L - \delta| \quad (13)$$

The azimuth angle ϕ is uniquely determined by its sine and cosine, given in Equations (14) and (15):

$$\sin \phi = \sin H \cos \delta / \cos \beta \quad (14)$$

$$\cos \phi = (\cos H \cos \delta \sin L - \sin \delta \cos L) / \cos \beta \quad (15)$$

Example 1. Calculate the position of the sun in the example city of Table 1 for July 21 at noon solar time.

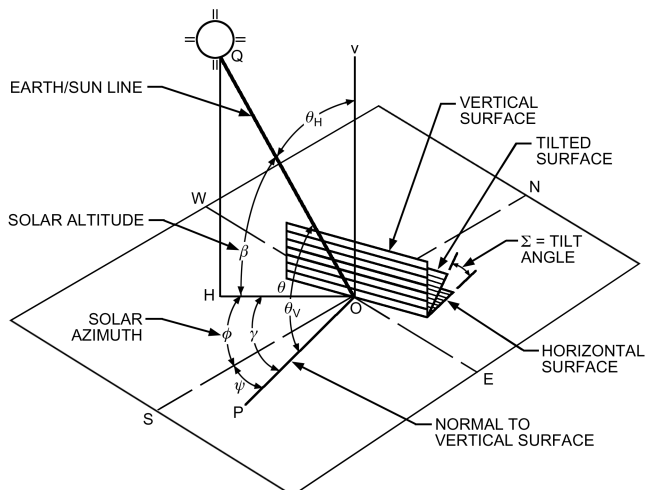


Fig. 3 Solar Angles for Vertical and Horizontal Surfaces

Solution: From Table 1, the example city is at latitude $L = 33.64^\circ$ N. From Table 2 or Equation (10), declination $\delta = 20.44^\circ$. Solar altitude is given by Equation (13):

$$\beta = 90 - |33.64 - 20.44| = 76.80^\circ$$

At solar noon, the sun is due south, so the azimuth angle ϕ is simply 0° .

Example 2. Perform the same calculation as in Example 1, but for 3:00 PM eastern daylight saving time.

Solution: Compared to Example 1, a few extra steps are required to calculate AST. From Table 1, for the example city, LON = 84.43° W = -84.43° E and TZ = -5.00. Also, from Table 2 or Equation (5), ET = -6.4 min. Then, from Equation (8):

$$\text{LSM} = 15(-5.00) = -75^\circ$$

Because 3 PM daylight saving time is 2 PM standard time, or hour 14, Equation (7) leads to

$$\text{AST} = 14 - 6.4/60 + [(-84.43) - (-75)]/15 = 13.27 \text{ h}$$

Then, from Equation (11):

$$H = 15(13.27 - 12) = 18.97^\circ$$

Solar altitude is given by Equation (12), using the same latitude and declination as in Example 1:

$$\begin{aligned} \sin \beta &= \cos(33.64^\circ) \cos(20.44^\circ) \cos(18.97^\circ) \\ &\quad + \sin(33.64^\circ) \sin(20.44^\circ) = 0.931 \end{aligned}$$

Therefore, $\beta = 68.62^\circ$.

Solar azimuth is obtained through Equations (14) and (15):

$$\sin \phi = \sin(18.97^\circ) \cos(20.44^\circ) / \cos(68.62^\circ) = 0.836$$

$$\cos \phi = [\cos(18.97^\circ) \cos(20.44^\circ) \sin(33.64^\circ) \\ - \sin(20.44^\circ) \cos(33.64^\circ)] / \cos(68.62^\circ) = 0.549$$

Therefore, $\phi = 56.69^\circ$.

Air Mass

The relative air mass m is the ratio of the mass of atmosphere in the actual earth/sun path to the mass that would exist if the sun were directly overhead. Air mass is solely a function of solar altitude β and is obtained from (Kasten and Young 1989)

$$m = 1 / [\sin \beta + 0.50572(6.07995 + \beta)^{-1.6364}] \quad (16)$$

where β is expressed in degrees.

Clear-Sky Solar Radiation

Solar radiation on a clear day is defined by its beam (direct) and diffuse components. The direct component represents the part of solar radiation emanating directly from the solar disc, whereas the diffuse component accounts for radiation emanating from the rest of the sky. These two components are calculated as

$$E_b = E_o \exp[-\tau_b m^{ab}] \quad (17)$$

$$E_d = E_o \exp[-\tau_d m^{ad}] \quad (18)$$

where

E_b = beam normal irradiance (measured perpendicularly to rays of the sun)

E_d = diffuse horizontal irradiance (measured on horizontal surface)

E_o = extraterrestrial normal irradiance [Equation (4) or Table 2]

m = air mass [Equation (16)]

τ_b and τ_d = beam and diffuse optical depths (τ_b and τ_d are more correctly termed pseudo-optical depths, because optical depth refers to an air mass coefficient without exponentiation; "optical depth" is used here for convenience.)

ab and ad = beam and diffuse air mass exponents

Values of τ_b and τ_d are location-specific and vary during the year. They embody the dependence of clear-sky solar radiation on

local conditions, such as elevation, precipitable water, aerosols, ozone, and surface reflectance. Their average values were determined through ASHRAE research project RP-1847 (Roth 2021), and are tabulated for the 21st day of each month for all the locations in the tables of climatic design conditions. Values for other days of the year should be found by interpolation.

Air mass exponents ab and ad are correlated to τ_b and τ_d through the following empirical relationships:

$$ab = 1.454 - 0.406 \tau_b - 0.268 \tau_d + 0.021 \tau_b \tau_d \quad (19)$$

$$ad = 0.507 + 0.205 \tau_b - 0.080 \tau_d - 0.190 \tau_b \tau_d \quad (20)$$

Equations (17) to (20) describe a simple parameterization of a sophisticated broadband radiation model and provide accurate predictions of E_b and E_d , even at sites where the atmosphere is very hazy or humid most of the time.

Example 3. Calculate clear-sky beam and diffuse solar irradiance in the example city of Table 1 for July 21 at noon solar time. Note that Table 1 already lists clear-sky beam and diffuse solar irradiance for solar noon. Calculations are shown here to illustrate the application of the method.

Solution: From Example 1, at solar noon on July 21 in the example city, solar altitude is $\beta = 76.80^\circ$. From Equation (16):

$$m = 1/[\sin(76.80^\circ) + 0.50572(6.07995 + 76.80)^{-1.6364}] = 1.027$$

From Table 1, the beam and diffuse optical depths for the example city in July are $\tau_b = 0.515$ and $\tau_d = 2.066$. From Table 2 or Equation (4), normal extraterrestrial irradiance on July 21 is $E_o = 420 \text{ Btu/h}\cdot\text{ft}^2$. Then, from Equations (19) and (20)

$$\begin{aligned} ab &= 1.454 - 0.406 \times 0.515 - 0.268 \times 2.066 + 0.021 \times 0.515 \times 2.066 \\ &= 0.714 \end{aligned}$$

$$\begin{aligned} ad &= 0.507 + 0.205 \times 0.515 - 0.080 \times 2.066 - 0.190 \times 0.515 \times 2.066 \\ &= 0.245 \end{aligned}$$

and from Equations (17) and (18),

$$E_b = 420 \exp(-0.515 \times 1.027^{0.714}) = 249 \text{ Btu/h}\cdot\text{ft}^2$$

$$E_d = 420 \exp(-2.066 \times 1.027^{0.245}) = 53 \text{ Btu/h}\cdot\text{ft}^2$$

These are the values listed for “Ebn at Noon” and “Edn at Noon” in Table 1.

Example 4. Perform the same calculation as in Example 3, but for 3 PM eastern daylight saving time.

Solution: This is the same calculation as in the solution of Example 3, but using the solar altitude $\beta = 68.62^\circ$ calculated in Example 2 (ab and ad are unchanged from Example 3):

$$m = 1/[\sin(68.62^\circ) + 0.50572(6.07995 + 68.62)^{-1.6364}] = 1.073$$

$$E_b = 420 \exp(-0.515 \times 1.073^{0.714}) = 244 \text{ Btu/h}\cdot\text{ft}^2$$

$$E_d = 420 \exp(-2.066 \times 1.073^{0.245}) = 51 \text{ Btu/h}\cdot\text{ft}^2$$

3. TRANSPOSITION TO RECEIVING SURFACES OF VARIOUS ORIENTATIONS

Calculations developed in the previous section are chiefly concerned with estimating clear-sky solar irradiance either normal to the rays of the sun (for the direct beam component) or on a horizontal surface (for the diffuse component). However, in many circumstances, calculation of clear-sky solar irradiance is required on surfaces of arbitrary orientations. Receiving surfaces can be vertical (e.g., walls and windows) or tilted (e.g., skylights or active solar devices). This section describes **transposition models** that enable calculating solar irradiance on any surface, knowing beam normal and diffuse horizontal irradiance.

Table 4 Surface Orientations and Azimuths, Measured from South

Orientation	N	NE	E	SE	S	SW	W	NW
Surface azimuth ψ	180°	-135°	-90°	-45°	0	45°	90°	135°

Solar Angles Related to Receiving Surfaces

The orientation of a receiving surface is best characterized by its tilt angle and its azimuth, shown in Figure 3. The tilt angle Σ (also called **slope**) is the angle between the surface and the horizontal plane. Its value lies between 0 and 180°. Most often, slopes are between 0° (horizontal) and 90° (vertical). Values above 90° correspond to surfaces facing the ground. The surface azimuth ψ is defined as the displacement from south of the projection, on the horizontal plane, of the normal to the surface. Surfaces that face west have a positive surface azimuth; those that face east have a negative surface azimuth. Surface azimuths for common orientations are summarized in Table 4. Note that, in this chapter, surface azimuth is defined as relative to south in both the northern and southern hemispheres. Other presentations and software use relative-to-north or relative-to-equator; care is required.

The surface-solar azimuth angle γ is defined as the angular difference between the solar azimuth ϕ and the surface azimuth ψ :

$$\gamma = \phi - \psi \quad (21)$$

Values of γ greater than 90° or less than -90° indicate that the surface is in the shade.

Finally, the angle between the line normal to the irradiated surface and the earth-sun line is called the angle of incidence θ . It is important in fenestration, load calculations, and solar technology because it affects the intensity of the direct component of solar radiation striking the surface and the surface's ability to absorb, transmit, or reflect the sun's rays. Its value is given by

$$\cos \theta = \cos \beta \cos \gamma \sin \Sigma + \sin \beta \cos \Sigma \quad (22)$$

Note that for vertical surfaces ($\Sigma = 90^\circ$) Equation (22) simplifies to

$$\cos \theta = \cos \beta \cos \gamma \quad (23)$$

whereas for horizontal surfaces ($\Sigma = 0^\circ$) it simplifies to

$$\theta = 90 - \beta \quad (24)$$

Example 5. For the example city of Table 1 on July 21 at 3 PM eastern daylight saving time, find the angle of incidence at a vertical widow facing 60° west of south.

Solution: The azimuth of the receiving surface is $\psi = +60^\circ$. According to Example 2, the solar azimuth angle is $\phi = 56.69^\circ$. Then, Equation (21) gives the surface-solar azimuth angle as

$$\gamma = 56.69^\circ - 60^\circ = -3.31^\circ$$

Still from Example 2, the solar altitude angle is $\beta = 68.62^\circ$. Equation (23) leads to

$$\cos \theta = \cos(68.62^\circ) \cos(-3.31^\circ) = 0.364$$

Therefore, $\theta = 68.66^\circ$.

Example 6. For the same conditions as in Example 5, find the angle of incidence at a skylight tilted at 30° and facing 60° west of south.

Solution: The azimuth of the receiving surface is still $\psi = +60^\circ$, but its slope is $\Sigma = 30^\circ$. Other angles are unchanged from Example 5. Equation (22) now applies:

$$\cos \theta = \cos(68.62^\circ) \cos(-3.31^\circ) \sin(30^\circ) + \sin(68.62^\circ) \cos(30^\circ) = 0.988$$

which leads to $\theta = 8.74^\circ$.

Calculation of Clear-Sky Solar Irradiance Incident on Receiving Surface

The total clear-sky irradiance E_t reaching the receiving surface is the sum of three components: the beam component $E_{t,b}$ originating from the solar disc; the diffuse component $E_{t,d}$, originating from the sky dome; and the ground-reflected component $E_{t,r}$ originating from the ground in front of the receiving surface. Thus,

$$E_t = E_{t,b} + E_{t,d} + E_{t,r} \quad (25)$$

Only a simple method for computing all the factors on the right side of Equation (25) is presented here. More elaborate methods, particularly with regard to the calculating the diffuse component, can be found in Gueymard (1987) and Perez et al. (1990).

Beam Component. The beam component is obtained from a straightforward geometric relationship:

$$E_{t,b} = E_b \cos \theta \quad (26)$$

where θ is the angle of incidence defined in Equation (22). This relationship is valid only when $\cos \theta > 0$ and the sun is not shaded (e.g., by an adjacent building); otherwise, $E_{t,b} = 0$.

Diffuse Component. The diffuse component is more difficult to estimate because of the anisotropic nature of diffuse radiation: some parts of the sky, such as the circumsolar disc or the horizon, tend to be brighter than the rest of the sky, which makes the development of a simplified model challenging. The model developed by Hay and Davies (1980) has been shown to work well, at least for $\Sigma \leq 90^\circ$, while being simple enough. It introduces an anisotropy index AI given by:

$$AI = E_b/E_o \quad (27)$$

where E_b is the beam normal irradiance and E_o is the normal extraterrestrial irradiance (Equation [4], or Table 2). Assuming no significant shading of the sky, the diffuse irradiance on the surface is

$$E_{t,d} = E_d \{AI \times R_b + (1 - AI)(1 + \cos \Sigma)/2\} \quad (28)$$

where R_b is given by

$$R_b = \cos \theta / \sin \beta \quad (29)$$

with θ the angle of incidence and β the elevation of the sun. R_b should be set to zero whenever the sun is below the horizon ($\beta < 0$) or the incidence angle θ exceeds 90° (that is, the sun is behind the surface).

Ground-Reflected Component. Assuming an infinite foreground and no shading that could affect the incident radiation on it, the ground-reflected irradiance for surfaces of all orientations is given by

$$E_{t,r} = (E_b \sin \beta + E_d) \rho_g \frac{1 - \cos \Sigma}{2} \quad (30)$$

where ρ_g is the ground albedo (or hemispherical reflectance), often taken to be 0.2 for a typical mixture of ground surfaces. Table 5 provides estimates of ρ_g for other surfaces, including cases when snow is present.

Example 7. Find the direct, diffuse, and ground-reflected components of clear-sky solar irradiance on the window in Example 5.

Solution: The clear-sky beam normal irradiance E_b and diffuse horizontal irradiance E_d were calculated in Example 4 as $E_b = 244 \text{ Btu/h}\cdot\text{ft}^2$ and $E_d = 51 \text{ Btu/h}\cdot\text{ft}^2$, respectively. Example 2 provided the solar altitude as $\beta = 68.62^\circ$, and Example 5 provided the angle of incidence as $\theta = 68.66^\circ$. The surface slope is $\Sigma = 90^\circ$, and the ground albedo is assumed to be 0.2. The extraterrestrial irradiance, from Example 4, is

Table 5 Albedo of Foreground Surfaces

Foreground Surface	Albedo
Water (near normal incidences)	0.07
Coniferous forest (winter)	0.07
Asphalt, new	0.05
weathered	0.10
Bituminous and gravel roof	0.13
Dry bare ground	0.2
Weathered concrete	0.2 to 0.3
Green grass	0.26
Dry grassland	0.2 to 0.3
Desert sand	0.4
Light building surfaces	0.6
Snow-covered surfaces:	
Typical city center	0.2
Typical urban site	0.4
Typical rural site	0.5
Isolated rural site	0.7

Source: Adapted from Thevenard and Haddad (2006).

$E_o = 420 \text{ Btu/h}\cdot\text{ft}^2$. Substituting these values into Equations (26) to (30) leads to

$$E_{t,b} = 244 \cos(68.66^\circ) = 89 \text{ Btu/h}\cdot\text{ft}^2$$

$$AI = 244 / 420 = 0.582$$

$$R_b = \cos(68.66^\circ) / \sin(68.62^\circ) = 0.391$$

$$E_{t,d} = 51 \times (0.582 \times 0.391 + (1 - 0.582) \times (1 + \cos(90^\circ)) / 2) = 22 \text{ Btu/h}\cdot\text{ft}^2$$

$$E_{t,r} = [244 \sin(68.62^\circ) + 51] \times 0.2 \times [1 - \cos(90^\circ)] / 2 = 28 \text{ Btu/h}\cdot\text{ft}^2$$

Example 8. Find the direct, diffuse and ground-reflected components of clear-sky solar irradiance on the skylight in Example 6.

Solution: This example uses the same values as Example 7, except that the surface slope is $\Sigma = 30^\circ$ and the angle of incidence, calculated in Example 6, is $\theta = 8.74^\circ$. The anisotropy index AI is unchanged. The irradiance components on the surface are then calculated from Equations (26), (28), (29) and (30):

$$E_{t,b} = 244 \cos(8.74^\circ) = 241 \text{ Btu/h}\cdot\text{ft}^2$$

$$R_b = \cos(8.74^\circ) / \sin(68.62^\circ) = 1.061$$

$$E_{t,d} = 51 \times (0.582 \times 1.061 + (1 - 0.582) \times (1 + \cos(30^\circ)) / 2) = 51 \text{ Btu/h}\cdot\text{ft}^2$$

$$E_{t,r} = [244 \sin(68.62^\circ) + 51] \times 0.2 \times (1 - \cos(30^\circ)) / 2 = 4 \text{ Btu/h}\cdot\text{ft}^2$$

4. GENERATING DESIGN-DAY DATA

This section provides procedures for generating 24 h temperature data sequences suitable as input to many HVAC analysis methods, including the radiant time series (RTS) cooling load calculation procedure described in Chapter 18.

Temperatures. Table 6 gives a normalized daily temperature profile in fractions of daily temperature range. Recent research projects RP-1363 (Hedrick 2009) and RP-1453 (Thevenard 2009) have shown that this profile is representative of both dry-bulb and wet-bulb temperature variation on typical design days. To calculate hourly temperatures, subtract the Table 6 fraction of the dry- or wet-bulb daily range from the dry- or wet-bulb design temperature (limiting by saturation in the case of the wet-bulb). This procedure is applicable to annual or monthly data and is shown in Example 9. Table 7 specifies the input values to be used for generating several design-day types.

Because daily temperature variation is driven by heat from the sun, the profile in Table 6 is, strictly speaking, specified in terms of solar time. Typical HVAC calculations (e.g., hourly cooling loads) are performed in local time, reflecting building operation schedules. The difference between local and solar time can easily be 1 or 2 h, depending on site longitude and whether daylight saving time is in effect. This difference can be included by accessing the temperature profile using apparent solar time (AST) calculated with Equation (7), as shown in Example 9.

Additional Moist-Air Properties. Once hourly dry-bulb and wet-bulb temperatures are known, additional moist air properties (e.g., dew-point temperature, humidity ratio, enthalpy) can be derived using the psychrometric chart, equations in Chapter 1, or psychrometric software.

Example 9. Deriving Hourly Design-Day Temperatures. Calculate hourly temperatures for the example city of Table 1 for a July dry-bulb design day using the 5% design conditions.

Solution: From Table 1, the July 5% dry-bulb design conditions for the example city are DB = 91.6°F and MCWB = 74.3°F. Daily range values are MCDBR = 20.2°F and MCWBR = 6.1°F. Daylight saving time is in effect for the example city in July. Apparent solar time (AST) for hour 1 local daylight saving time (LDT) is -0.73. The nearest hour to the AST is 23, yielding a Table 6 profile value of 0.75. Then $t_{db,1} = 91.6 - 0.75 \times 20.2 = 76.5^\circ\text{F}$. Similarly, $t_{wb,1} = 74.3 - 0.75 \times 6.1 = 69.7^\circ\text{F}$. With psychrometric formulas, derive $t_{dp,1} = 66.7^\circ\text{F}$. Table 8 shows results of this procedure for all 24 h.

5. ESTIMATION OF DEGREE-DAYS

Monthly Degree-Days

The tables of climatic design conditions in this chapter list heating and cooling degree-days (bases 50 and 65°F). Although 50 and 65°F represent the most commonly used bases for the calculation of degree-days, calculation to other bases may be necessary. With that goal in mind, the tables also provide two parameters (monthly average temperature \bar{T} , and standard deviation of daily average temperature s_d) that enable estimation of degree-days to any base with reasonable accuracy.

The calculation method was established by Schoenau and Kehrig (1990). Heating degree days HDD_b to base T_b are expressed as

$$\text{HDD}_b = Ns_d [Z_b F(Z_b) + f(Z_b)] \quad (31)$$

where N is the number of days in the month and Z_b is the difference between monthly average temperature \bar{T} and base temperature T_b , normalized by the standard deviation of the daily average temperature s_d :

$$Z_b = \frac{T_b - \bar{T}}{s_d} \quad (32)$$

Function f is the normal (Gaussian) probability density function with mean 0 and standard deviation 1, and function F is the equivalent cumulative normal probability function:

$$f(Z) = \frac{1}{\sqrt{2\pi}} \exp\left(-\frac{Z^2}{2}\right) \quad (33)$$

$$F(Z) = \int_{-\infty}^Z f(z) dz \quad (34)$$

Both f and F are readily available as built-in functions in many scientific calculators or spreadsheet programs, so their manual calculation is rarely warranted.

Cooling degree days CDD_b to base T_b are calculated by the same equation:

$$\text{CDD}_b = Ns_d [Z_b F(Z_b) + f(Z_b)] \quad (35)$$

except that Z_b is now expressed as

$$Z_b = \frac{\bar{T} - T_b}{s_d} \quad (36)$$

Alternative Equations. The following formulas from ISO Standard 15927-6 give results very similar to Equations (32) and (36) but are somewhat simpler:

$$\text{HDD}_b = \frac{N(T_b - \bar{T})}{1 - \exp(-\sqrt{2\pi}(T_b - \bar{T})/s_d)} \quad (37)$$

$$\text{CDD}_b = \frac{N(\bar{T} - T_b)}{1 - \exp(-\sqrt{2\pi}(\bar{T} - T_b)/s_d)} \quad (38)$$

When $\bar{T} = T_b$, the right-hand side of these equations become $Ns_d/\sqrt{2\pi}$.

Annual Degree-Days

Annual degree-days are simply the sum of monthly degree days over the twelve months of the year.

Example 10. Calculate heating and cooling degree-days (base 59°F) for the example city of Table 1 for the month of October.

Solution: For October in the example city, Table 1 provides $\bar{T} = 63.6^\circ\text{F}$ and $s_d = 7.07^\circ\text{F}$. For heating degree-days, Equation (32) provides $Z_b = (59 - 63.6)/7.07 = -0.651$. From a scientific calculator or a spreadsheet program $f(Z_b) = 0.323$, and $F(Z_b) = 0.258$. Equation (31) then gives

Table 6 Fraction of Daily Temperature Range

Time, h	Fraction	Time, h	Fraction	Time, h	Fraction
1	0.88	9	0.55	17	0.14
2	0.92	10	0.38	18	0.24
3	0.95	11	0.23	19	0.39
4	0.98	12	0.13	20	0.50
5	1.00	13	0.05	21	0.59
6	0.98	14	0.00	22	0.68
7	0.91	15	0.00	23	0.75
8	0.74	16	0.06	24	0.82

Table 7 Input Sources for Design-Day Generation

Design Day Type	Design Conditions	Daily Ranges	Limits
Dry-bulb			
Annual	0.4, 1, or 2% annual cooling DB/MCWB	Hottest month 5% DB MCDBR/MCWBR	Hourly wet-bulb temp. = min(dry-bulb temp., wet-bulb temp.)
Monthly	0.4, 2, 5, or 10% DB/MCWB for month	5% DB MCDBR/MCWBR for month	
Wet-bulb			
Annual	0.4, 1, or 2% annual cooling WB/MCDB	Hottest month 5% WB MCDBR/MCWBR	Hourly dry-bulb temp. = max(dry-bulb temp., wet-bulb temp.)
Monthly	0.4, 2, 5, or 10% WB/MCDB for month	5% WB MCDBR/MCWBR for month	

Table 8 Derived Hourly Temperatures for Example City for July for 5% Design Conditions, °F

Hour (LDT)	t_{db}	t_{wb}	t_{dp}	Hour (LDT)	t_{db}	t_{wb}	t_{dp}
1	76.5	69.7	66.7	13	87.0	72.9	66.9
2	75.0	69.3	66.7	14	89.0	73.5	67.0
3	73.8	68.9	66.7	15	90.6	74.0	67.1
4	73.0	68.7	66.7	16	91.6	74.3	67.1
5	72.4	68.5	66.7	17	91.6	74.3	67.1
6	71.8	68.3	66.8	18	90.4	73.9	67.1
7	71.4	68.2	66.8	19	88.8	73.4	67.0
8	71.8	68.3	66.8	20	86.8	72.8	66.9
9	73.2	68.7	66.7	21	83.7	71.9	66.8
10	76.7	69.8	66.7	22	81.5	71.3	66.8
11	80.5	70.9	66.8	23	79.7	70.7	66.8
12	83.9	72.0	66.8	24	77.9	70.2	66.7

LDT = Local daylight saving time.

$$\text{HDD}_{59} = 31 \times 7.07(-0.651 \times 0.258 + 0.323) = 34.0^\circ\text{F-day}$$

For cooling degree-days, $Z_b = 0.651$. Note that $f(-Z_b) = f(Z_b)$ and $F(-Z_b) = 1 - F(Z_b)$, hence

$$f(Z_b) = 0.323 \quad \text{and} \quad F(Z_b) = 0.742$$

and

$$\text{CDD}_{59} = 31 \times 7.07(0.651 \times 0.742 + 0.323) = 176.6^\circ\text{F-day}$$

For most stations, the monthly degree-days calculated with this method are within 9°F-day of the observed values.

6. REPRESENTATIVENESS OF DATA AND SOURCES OF UNCERTAINTY

Representativeness of Data

The climatic design information in this chapter was obtained by direct analysis of observations from the indicated locations. Design values reflect an estimate of the cumulative frequency of occurrence of the weather conditions at the recording station, either for single or jointly occurring elements, for several years into the future. Several sources of uncertainty affect the accuracy of using the design conditions to represent other locations or periods.

The most important of these factors is spatial representativeness. Most of the observed data for which design conditions were calculated were collected from airport observing sites, the majority of which are flat, grassy, open areas, away from buildings and trees or other local influences. Temperatures recorded in these areas may be significantly different from built-up areas where the design conditions are being applied. For example, the maximum urban heat island intensity may be 18°F or more (Oke 1987), although intraurban variability is typically quite large. Urban microclimate is affected by the three-dimensional density of building construction, usually represented by the ratio of building height to street width (H/W); by type and extent of plant cover; and by anthropogenic heat emissions from buildings and vehicles. Significant variations can also occur with changes in local elevation, even if elevations differ by a few hundred feet, or in the vicinity of large bodies of water. It should be emphasized that such variations are not constant in time: intraurban differences in temperature and humidity fluctuate not only in predictable diurnal patterns, but also in response to changes in synoptic conditions and wind direction. Urban heat islands, for example, are typically prominent on clear nights with little or no wind, and are weaker or nonexistent in windy conditions and during daytime. Therefore, judgment must always be used in assessing the representativeness of the design conditions. Consult an applied climatologist regarding estimating design conditions for locations not listed in this chapter. For online references to applied climatologists

Table 9 Locations Representing Various Climate Types

Cold Snow Forest	Dry	Warm Rainy	Tropical Rainy
Portland, ME	Amarillo, TX	Huntsville, AL	Key West, FL
Grand Island, NE	Bakersfield, CA	Wilmington, NC	West Palm Beach, FL
Minot, ND	Sacramento, CA	Portland, OR	
Indianapolis, IN	Phoenix, AZ	Quillayute, WA	

in the United States, see wcdirectory.ametsoc.org/certified-consulting-meteorologists; in Canada, consult cmos.ca/client/roster/clientRosterView.html?clientRosterId=190.

Depending on a site's specific geographic location and setting (e.g., proximity to large body of water or hills), the data in this chapter for the nearest weather station may not be representative of the actual climate experienced at the project site. In these instances, it may be beneficial to obtain climate data using procedures developed by ASHRAE research project RP-1561 (Qiu et al. 2016). The methodologies provide a protocol for using state-of-the-art mesoscale modeling techniques to derive meteorological conditions specific to the study area. The research project included the methodology based on the Weather Research and Forecasting (WRF) model designed to develop site-specific climate data where standard weather stations are unavailable or not representative of site conditions. The methodology was evaluated by using observations in various geographic regions, including coastal, mountain valley, mountain plateau, and major cities. A simplified procedure was developed; it is freely available at klimaat.github.io/emspy/.

The underlying data also depend on the method of observation. During the 1990s, most data gathering in the United States and Canada was converted to automated systems designated either an automated surface observation system (ASOS) or an automated weather observing system (AWOS). This change improved completeness and consistency of available data. However, changes have resulted from the inherent differences in type of instrumentation, instrumentation location, and processing procedures between the prior manual systems and ASOS. These effects were investigated in ASHRAE research project RP-1226 (Belcher and DeGaetano 2004). Comparison of one-year ASOS and manual records revealed some biases in dry-bulb temperature, dew-point temperature, and wind speed. These biases are judged to be negligible for HVAC engineering purposes; the tabulated design conditions in this chapter were derived from mixed automated and manual data as available. Changes in the location of the observing instruments often have a larger effect than changes in instrumentation.

Weather conditions vary from year to year and, to some extent, from decade to decade because of the inherent variability of climate. Similarly, values representing design conditions vary depending on the period of record used in the analysis. Thus, because of short-term climatic variability, there is always some uncertainty in using design conditions from one period to represent another period. Typically, values of design dry-bulb temperature vary less than 2°F from decade to decade, but larger variations can occur. Differing periods used in the analysis can lead to differences in design conditions between nearby locations at similar elevations. Design conditions may show trends in areas of increasing urbanization or other regions experiencing extensive changes to land use. Longer-term climatic change brought by human or natural causes may also introduce trends into design conditions. This is discussed further in the section on Effects of Climate Change.

Wind speed and direction are very sensitive to local exposure features such as terrain and surface cover. The original wind data used to calculate the wind speed and direction design conditions in Table 1 are often representative of a flat, open exposure, such as at airports. Wind engineering methods, as described in Chapter 24, can be used to account for exposure differences between airport and

building sites. This is a complex procedure, best undertaken by an experienced applied climatologist or wind engineer with knowledge of the exposure of the observing and building sites and surrounding regions.

Uncertainty from Variation in Length of Record

ASHRAE research project RP-1171 (Hubbard et al. 2004) investigated the uncertainty associated with the climatic design conditions in the 2001 *ASHRAE Handbook—Fundamentals*. The main objectives were to determine how many years are needed to calculate reliable design values and to look at the frequency and duration of episodes exceeding the design values.

Design temperatures in the 1997 and 2001 editions were calculated for locations for which there were at least 8 years of sufficient data; the criterion for using 8 years was based on unpublished work by TC 4.2. RP-1171 analyzed data records from 14 U.S. locations (Table 9) representing four different climate types. The dry-bulb temperatures corresponding to the five annual percentile design temperatures (99.6, 99, 0.4, 1, and 2%) from the 33-year period 1961–1993 (period used for the 2001 edition's U.S. stations) were calculated for each location. The temperatures corresponding to the same percentiles for each contiguous subperiod ranging from 1 to 33 years in length was calculated, and the standard deviation of the differences between the resulting design temperature from each subperiod and the entire 33-year period was calculated. For instance, for a 10-year period, the dry-bulb values corresponding to each of the 23 subperiods 1961–1970, 1962–1971, ... 1984–1993 were calculated and the standard deviation of differences with the dry-bulb value for the same percentile from the 33-year period calculated. The standard deviation values represent a measure of uncertainty of the design temperatures relative to the design temperature for the entire period of record.

The results for the five annual percentiles are summarized in Figures 4A to 4E, each of which shows how the uncertainty (the average standard deviation for each of the locations in each climate type) varies with length of period.

To the degree that the differences used to calculate the standard deviations are distributed normally, the short-period design temperatures can be expected to lie within one standard deviation of the long-term design temperature 68% of the time. For example, from Figure 4A, the uncertainty for the cold snow forest for a 1-year period is 6.5°F. This can be interpreted that the probability is 68% that the difference in a 99.6% dry-bulb in any given year will be within 6.5°F of the long-term 99.6% dry-bulb. Similarly, there is a 68% probability that the 99.6% dry-bulb from any 10-year period will be within 1.8°F of the long-term value for a location of the cold snow forest climate type.

The uncertainty for the cold season is higher than for the warm season. For example, the uncertainty for the 99.6% dry-bulb for a 10-year period ranges from 1.1 to 1.8°F for the five climate types, whereas the uncertainty for the 0.4% dry-bulb for a 10-year period ranges from 0.7 to 1.1°F.

A variety of other general characteristics of uncertainty are evident from an inspection of Figure 4. For example, the highest uncertainty of any climate type for a 10-year period is 2.0°F for the cold snow forest 99% dry-bulb case. The smallest uncertainty is 0.4°F for the tropical rainy 1% and 2% dry-bulb cases.

Based on these results, it was concluded that using a minimum of 8 years of data would provide reliable (within $\pm 1.8^{\circ}\text{F}$) climatic design calculations for most stations.

Effects of Climate Change

The evidence is unequivocal that the climate system is warming globally (IPCC 2015). The most frequently observed effects relate to increases in average, and to some degree, extreme temperatures.

This is partly shown by the results of an analysis of design conditions conducted as part of calculating the values for the 2009 edition of this chapter (Thevenard 2009). For 1274 observing sites

worldwide with suitably complete data from 1977 to 2006, selected design conditions were compared between the period 1977–1986 and 1997–2006. The results, averaged over all locations, are as follows:

- The 99.6% annual dry-bulb temperature increased 2.74°F
- The 0.4% annual dry-bulb increased 1.42°F
- Annual dew point increased by 0.99°F
- Heating degree-days (base 65°F) decreased by $427^{\circ}\text{F}\text{-days}$
- Cooling degree-days (base 50°F) increased by $245^{\circ}\text{F}\text{-days}$

Although these results are consistent with general warming of the world climate system, there are other effects that undoubtedly contribute, such as increased urbanization around many of the observing sites (airports, typically). There was no attempt in the analysis to determine the reasons for the changes.

A more recent study by Roth (2016), using stations used in the 2017 edition of this chapter, looked at trends for yearly average dry-bulb temperature and other quantities over the 1990 to 2014 period using statistical methods. The study showed that statistically significant increases in average dry-bulb temperature can be detected in only 24% of stations on an individual basis. However, trends become more apparent when stations are evaluated in groups. Stations were grouped in $5^{\circ}\times 5^{\circ}$ cells covering the globe. Of these cells, 38% showed an increase in average dry-bulb temperature, and 2% showed a decrease; 22% showed an increase in average dew-point temperature and 11% a decrease; finally, 26% showed an increase in average wet-bulb temperature, and 6% showed a decrease. Geographically, increases in average dry-bulb temperature were most visible throughout Europe, in China and southeast Asia, the eastern United States, southern South America, and southern Australia, and are typically in the range of 0.36 to 1.08°F per decade. Northern locations exhibited higher positive trends (above 1.8°F per decade). Dew-point temperature increases were most visible in eastern Europe, Atlantic Canada, and Indonesia, whereas decreases were experienced in the southern United States, South America, Mongolia, and southern China.

Regardless of the reasons for increases, the general approach of developing design conditions based on analysis of the recent record (26 years, in this case) was specifically adopted for updating the values in this chapter as a balance between accounting for long-term trends and the sampling variation caused by year-to-year variation. Although this does not necessarily provide the optimum predictive value for representing conditions over the next one or two decades, it at least has the effect of incorporating changes in climate and local conditions as they occur, as updates are conducted regularly using recent data. Meteorological services worldwide are considering the many aspects of this complex issue in the calculation of climate "normals" (averages, extremes, and other statistical summary information of climate elements typically calculated for a 30-year period at the end of each decade). Livezey et al. (2007) and WMO (2007) provide detailed analyses and recommendations in this regard.

Extrapolating design conditions to the next few decades based on observed trends should only be done with attention to the particular climate element and the regional and temporal characteristics of observed trends (Livezey et al. 2007).

Episodes Exceeding the Design Dry-Bulb Temperature

Design temperatures based on annual percentiles indicate how many hours each year on average the specific conditions will be exceeded, but do not provide any information on the length or frequency of such episodes. As reported by Hubbard et al. (2004), each episode and its duration for the locations in Table 9 during which the 2001 design conditions represented by the 99.6, 99, 0.4, 1, and 2% dry-bulb temperatures were exceeded (i.e., were more extreme) was tabulated and their frequency of occurrence analyzed. The measure

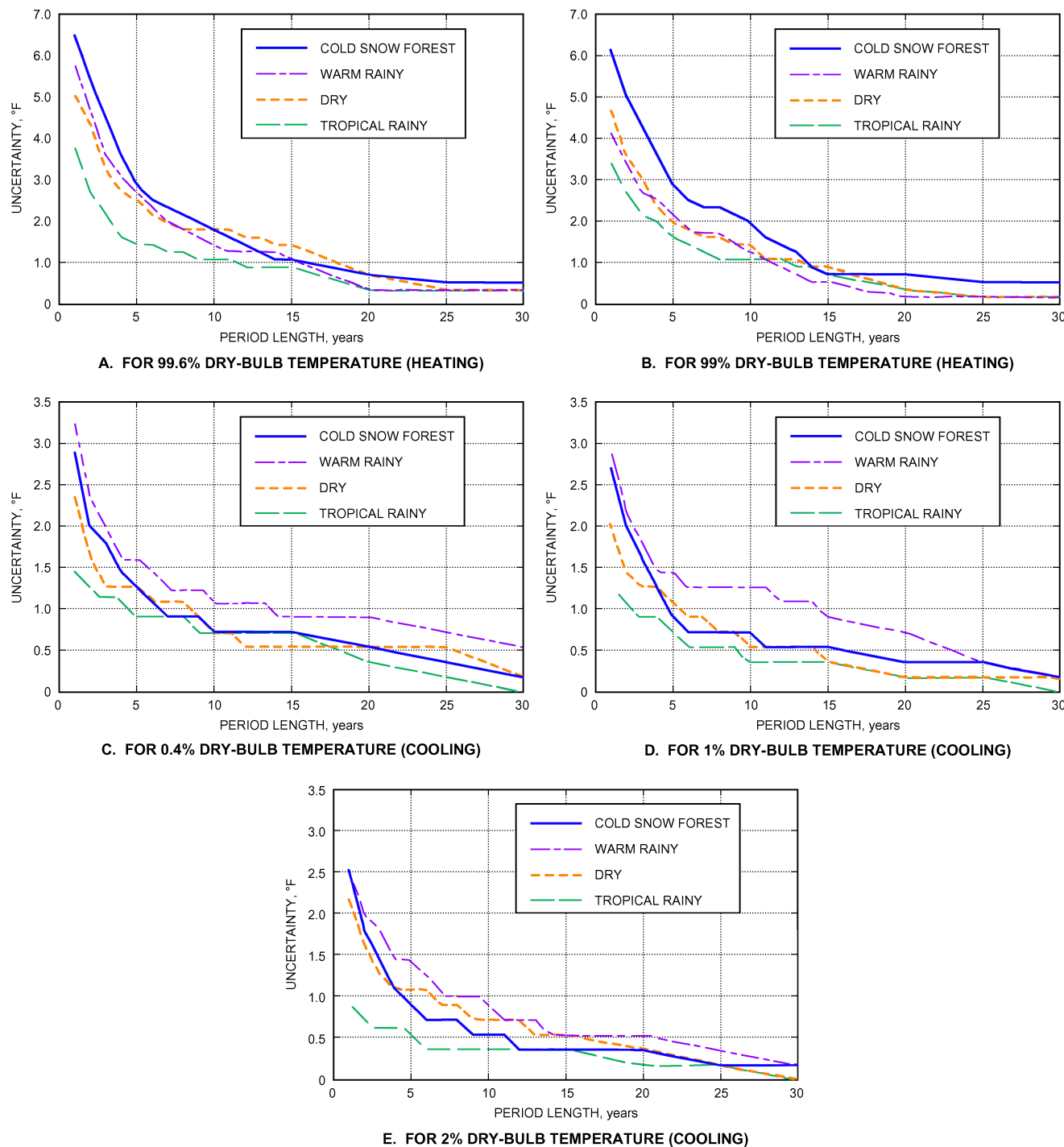


Fig. 4 Uncertainty versus Period Length for Various Dry-Bulb Temperatures, by Climate Type

of frequency is the average number of episodes per year or its reciprocal, the average period between episodes.

Cold- and warm-season results are presented in Figures 5A and 5B, respectively, for Indianapolis, IN, as a representative example. The duration for the 10-year period between episodes more extreme than the 99.6% design dry bulb is 37 h, and 62 h for the 99% design dry bulb. For the warm season, the 10-year period durations corresponding to the 0.4, 1, and 2% design dry bulb, are about 10, 12, and 15 h, respectively.

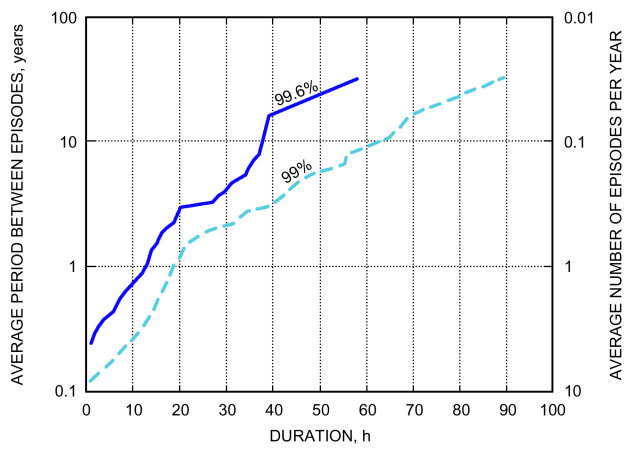
Although the results in Hubbard et al. (2004) varied somewhat among the locations analyzed, generally the longest cold-season episodes last days, whereas the longest warm-season episodes were always shorter than 24 h. These results were seen at almost all locations, and are general for the continental United States. The only exception was Phoenix, where the longest cold-season episodes were less than 24 h. This is likely the result of the southern latitude and dry climate, which produces a large daily temperature range, even in the cold season.

7. OTHER SOURCES OF CLIMATIC INFORMATION

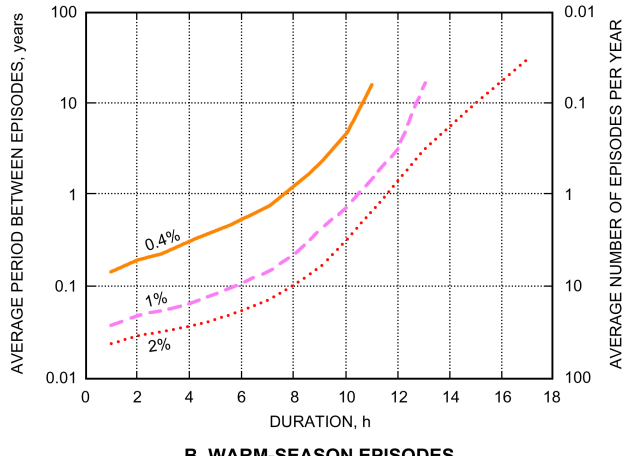
Joint Frequency Tables of Psychrometric Conditions

Design values in this chapter were developed by ASHRAE research project RP-1847 (Roth 2021). The frequency tables used to calculate the simple design conditions, and the joint frequency matrices used to calculate the coincident design conditions, are available in ASHRAE's Weather Data Viewer, which is now a web-based product (for details, see www.ashrae.org/technical-resources/bookstore/weather-data-center). The Weather Data Viewer gives users full access to the frequency tables and joint frequency matrices for all 9237 stations in the 2021 *ASHRAE Handbook—Fundamentals* via an easy-to-use web-based interface, and provides the following capabilities:

- Select a station by WMO number or region/country/state/name or by proximity to a given latitude and longitude.
- Retrieve design climatic conditions for a specified station, in SI or I-P units.
- Display frequency vectors and joint frequency matrices in the form of numerical tables.
- Display frequency distribution and the cumulative frequency distribution functions in graphical form.
- Display joint frequency functions in graphical form.
- Display the table of years and months used for the calculation.



A. COLD-SEASON EPISODES



B. WARM-SEASON EPISODES

Fig. 5 Frequency and Duration of Episodes Exceeding Design Dry-Bulb Temperature for Indianapolis, IN

- Display hourly binned dry-bulb temperature data.
- Calculate heating and cooling degree-days to any base, using the method of Schoenau and Kehrig (1990).

The **Engineering Weather Data CD** (NCDC 1999), an update of Air Force Manual 88-29, was compiled by the U.S. Air Force 14th Weather Squadron. This CD contains several tabular and graphical summaries of temperature, humidity, and wind speed information for hundreds of locations in the United States and around the world. In particular, it contains detailed joint frequency tables of temperature and humidity for each month, binned at 1°F and 3 h local time-of-day intervals. This CD is available from the National Centers for Environmental Information (NCEI): www.ncdc.noaa.gov/nespls/olstore.prod?prodnum=5005.

An online system which provides access to climate summary tables for worldwide locations is available from NCEI: gis.ncdc.noaa.gov/maps/ncei/summaries/global. This can be used as an aid in estimating design conditions for locations not available in the 2021 ASHRAE Handbook. Various parameters include temperature, dew point, relative humidity, sea level pressure, wind speed/direction, and cloud cover. For helpful information regarding usage of this GIS interface: gis.ncdc.noaa.gov/maps/ncei/help.

Degree Days and Climate Normals

Climate normals are three-decade averages of climatological variables, including temperature, precipitation, snowfall, snow depth, and degree-days.

The 1981 to 2010 climate normals for over 9800 United States locations are available online from NCEI: www.ncdc.noaa.gov/data-access/land-based-station-data/land-based-datasets/climate-normals/1981-2010-normals-data.

NCEI has additional online systems which provide station climate summaries of particular interest to engineering, energy, industry, and agricultural applications. The Supplemental Monthly Temperature Normals provide temperature statistics for various time periods and definitions of "normal": www.ncdc.noaa.gov/normals/PDFaccess/. The US Climate Atlas provides color-coded maps of temperature and precipitation, allowing the user to select a specific year or the long-term climatology: www.ncdc.noaa.gov/climateatlas/.

The Canadian Climate Normals (updated every 10 years; the most recent values are for the 1981–2010 period) can be found at climate.weather.gc.ca/climate_normals/index_e.html. This includes temperature, precipitation, snowfall, snow depth, degree-days, and other variables.

Typical Year Data Sets

Software used to simulate the annual energy performance of buildings often require a one-year data set (8760 h) of "typical" weather conditions. Many data sets in different record formats have been developed to meet this requirement and are generically called **Typical Meteorological Years (TMYs)**. The data are produced using an objective statistical algorithm to select the most typical month from the long-term record, and represent a typical, or "median", year with respect to weather-induced energy loads on a building. By construction, a TMY removes all weather extremes, and hence cannot represent design conditions.

The National Renewable Energy Laboratory's (NREL) has developed TMYs for the USA and other locations (nsrdb.nrel.gov/). These files contain gridded weather, solar radiation, and environmental TMY data, and are available through a visual and dynamic interface from maps.nrel.gov/nsrdb-viewer. The solar radiation data are derived from satellite observations, and the environmental data are down-scaled from the MERRA2 reanalysis data set derived from a large climate forecasting model (Sengupta et al., 2018). The grid spacing for this source of data is about 2.5 miles, and currently covers North America up to 60° N, as well as a part of South America down

to 21° S for the period 1998 to 2018. Some parts of South East Asia are also covered, albeit with a coarser spatial resolution and shorter time period. Various types of TMY data are available there, as well as each historical year within that time period, with anticipated annual updates. A set of older TMY files, called TMY3 (Wilcox and Marion 2008) and containing data for 1020 U.S. locations, is also available from rredc.nrel.gov/solar/old_data/nsrdb/1991-2005/tmy3/.

Canadian Weather Year for Energy Calculation (CWEC) files for 492 Canadian locations were developed for use with the National Energy Code of Canada for Buildings, using the TMY algorithm and software (climate.weather.gc.ca/prods_servs/engineering_e.html).

ASHRAE's International Weather for Energy Calculations (IWEC2) data set (Huang et al. 2014) contains typical-year weather data for 3012 international locations outdoor of the United States and Canada. The IWEC2s were developed through ASHRAE RP-1477, which used the same source of weather data (ISD; Smith et al. 2011) as used for the design condition tables in this chapter, but for a slightly earlier time period of 12 to 25 years ending in 2009. The IWEC2 data set is available on a DVD from the ASHRAE Climate Data Center at www.ashrae.org/resources--publications/book-store/climate-data-center#iweec; individual files and country sets are also available online from commercial resellers.

Observational Data Sets

For detailed designs, custom analysis of the most appropriate long-term weather record is best. National weather services are generally the best source of long-term observational data. The National Centers for Environmental Information (NCEI), in conjunction with U.S. Air Force and Navy partners in Asheville's Federal Climate Complex (FCC), developed the global Integrated Surface Data (Lott 2004; Smith et al. 2011) to address a pressing need for an integrated global database of hourly land surface climatological data. The database of over 25,000 stations contains hourly and some daily summary data from as early as 1900 (many stations beginning in the 1948–1973 timeframe), is operationally updated each day with the latest available data, and continues to be further integrated with various data sets from the United States and other countries to further expand the spatial and temporal coverage of the data. For a complete review of ISD and access to the data and products, go to www.ncdc.noaa.gov/isd or, for a GIS interface, gis.ncdc.noaa.gov/maps/ncei/cdo/hourly.

Additional climatic data are available from the NCEI Global Historical Climate Network (GHCN) summary of day and summary of month datasets: <https://www.ncdc.noaa.gov/data-access/land-based-station-data/land-based-datasets/global-historical-climatology-network-ghcn>. These datasets include data for various locations that do not have data available in ISD or in this chapter.

The National Solar Radiation Database (NSRDB) (nsrdb.nrel.gov/; www.ncdc.noaa.gov/data-access/land-based-station-data/land-based-datasets/solar-radiation) and Canadian Weather Energy and Engineering Data Sets (CWEEDS) (climate.weather.gc.ca/prods_servs/engineering_e.html) provide long-term hourly data, including solar radiation values for the United States and Canada. Previous versions of the NSRDB (rredc.nrel.gov/solar/old_data/nsrdb) required a modified solar radiation model because of the implementation of automated observing systems that do not report traditional cloud elements. The current NSRDB predictions of solar radiation (nsrdb.nrel.gov), mentioned earlier in the section on Typical Year Data Sets, do not rely on airport-based cloud observations anymore but rather on imagery from geosynchronous satellites. These files also contain related meteorological and environmental data and cover North America up to 60° North, and South America down to 20° South. The solar radiation data are derived from two GOES satellites and the environmental data are downscaled from the MERRA-2 reanalysis.

Considerable information about weather and climate services and data sets is available elsewhere online. Information supplementary to this chapter may also be posted on the ASHRAE Technical Committee 4.2 web site (tc0402.ashraetcs.org).

Reanalysis Data Sets

Reanalysis data sets are comprehensive time series of meteorological data obtained through combining observational data with numerical weather prediction models to produce synthesized snapshots of the state of the atmosphere over time. Reanalysis data sets normally span several decades and some cover the entire globe. They typically contain a very large number of climatic variables, at several heights, on a spatial grid with a resolution that currently spans 12 to 60 miles or more. These data sets are therefore very appealing as sources of engineering climatic data, particularly to obtain climatic time series in "data deserts" (i.e., vast areas of the world with no or few weather stations). Three particularly widely used global reanalysis data sets are CFS from NOAA (Saha et al. 2014), MERRA-2 from NASA (Gelaro et al. 2017), and ERA5 from ECMWF (ECMWF, 2019). Note that these data sets are very large and working with them requires substantial processing power and knowledge of specific tools to download and decode the highly compressed data files. Some commercial or free resources can assist in getting the data.

ASHRAE project RP-1745 (Roth 2019) studied the use of reanalysis data sets to calculate design climatic conditions or as input to building simulation software. The study found that when reanalysis data are used to compute climatic design conditions such as those found in Table 1, the results are generally well correlated with the values calculated from actual observations. Nevertheless, there is evidence of both a consistent bias in many of the conditions, along with an unacceptable level of station-by-station deviation between reanalysis and observations. In particular, reanalyses were found to be inadequate in regions with uneven topographic features or near large bodies of water.

Variables based on dry bulb temperature are typically better estimated than humidity-related variables, such as dew point or wet bulb temperature, which in turn are better estimated than wind, solar, or precipitation-based conditions. Also, more extreme conditions such as the 0.4% heating or cooling conditions are typically more challenging than simple climatic averages. The project also found that reanalyses suffer from similar weaknesses when used to generate weather files suitable for input to building energy simulation software: reanalysis weather files can lead to significant biases in estimated energy usage. This issue is amplified over the problem areas identified above.

The general conclusion is that, although reanalysis data sets show great potential, their output cannot be used directly for either calculating climatic design conditions, or as an input to an energy building simulation. Hence, caution should be exercised. It is advised to use the services of a qualified meteorologist to "nudge" the reanalysis data set closer to reality by applying a bias correction based on station or regional observational data, or by adjusting elevation-induced effects at locations with rapidly-changing terrain based on estimates of the vertical structure of the atmosphere. (See Chapter 6 of Roth [2019] for a brief survey of available methodologies and associated references.)

Another area where reanalysis models can prove useful is for filling gaps in observational datasets. The same nudging techniques described above should also be used.

Finally, a high-resolution mesoscale model (see results of RP-1561 [Qiu et al. 2016]) can be used to downscale the data. This downscaling works with a finer grid constrained to the reanalysis grid, and enables to better estimate the local conditions, and decrease the bias, by modeling physical phenomena with a higher

spatial and temporal resolution, for example in areas with rapidly changing elevation.

REFERENCES

- ASHRAE members can access *ASHRAE Journal* articles and ASHRAE research project final reports at technologyportal.ashrae.org. Articles and reports are also available for purchase by nonmembers in the online ASHRAE Bookstore at www.ashrae.org/bookstore.
- Belcher, B.N., and A.T. DeGaetano. 2004. Integration of ASOS weather data into building energy calculations with emphasis on model-derived solar radiation (RP-1226). ASHRAE Research Project, *Final Report*.
- Colliver, D.G., R.S. Gates, T.F. Burkes, and H. Zhang. 2000. Development of the design climatic data for the 1997 *ASHRAE Handbook—Fundamentals*. *ASHRAE Transactions* 106(1).
- ECMWF. 2019. Operational global reanalysis: progress, future directions and synergies with NWP. www.ecmwf.int/en/elibrary/18765-operational-global-reanalysis-progress-future-directions-and-synergies-nwp.
- Eskes, H., et al. 2015. Validation of reactive gases and aerosols in the MACC global analysis and forecast system. *Geoscientific Model Development* 8(11):3523–3543. www.geosci-model-dev.net/8/3523/2015/gmd-8-3523-2015-discussion.html.
- Gelaro, R., W. McCarty, M.J. Suarez, R. Todling, A. Molod, L. Takacs, C.A. Randles, et al. 2017. The modern-era retrospective analysis for research and applications, version 2 (MERRA-2). *Journal of Climate* 30:5419–5454.
- GHCN. 2015. *Global historical climatology network—Daily*. National Climatic Data Center, National Oceanic and Atmospheric Administration, Asheville, NC. www.ncdc.noaa.gov/ghcn-daily-description and ftp.ncdc.noaa.gov/pub/data/ghcn/daily/.
- GPCC. 2018. *GPCC full data monthly product version 2018*. Global Precipitation Climatology Centre, Deutscher Wetterdienst, Offenbach am Main, Germany. opendata.dwd.de/climate_environment/GPCC/html/fulldata-monthly_v2018_doi_download.html.
- GPCP. 2020. *GPCP version 2.3 combined precipitation data set*. GPCP Precipitation data provided by the NOAA/OAR/ESRL PSD, Boulder, CO, USA. www.esrl.noaa.gov/psd/data/gridded/data.gpcp.html.
- Gueymard, C.A. 1987. An anisotropic solar irradiance model for tilted surfaces and its comparison with selected engineering algorithms. *Solar Energy* 38:367–386. Erratum, *Solar Energy* 40:175 (1988).
- Gueymard, C.A. 2008. REST2: High performance solar radiation model for cloudless-sky irradiance, illuminance and photosynthetically active radiation—Validation with a benchmark dataset. *Solar Energy* 82:272–285.
- Gueymard, C.A., and D. Thevenard. 2009. Monthly average clear-sky broadband irradiance database for worldwide solar heat gain and building cooling load calculations. *Solar Energy* 83:1998–2018.
- Harriman, L.G., D.G. Colliver, and H.K. Quinn. 1999. New weather data for energy calculations. *ASHRAE Journal* 41(3):31–38.
- Hay, J.E., and Davies, J.A. 1980. Calculations of the solar radiation incident on an inclined surface. In J.E. Hay and T.K. Won, eds. *Proceedings of First Canadian Solar Radiation Data Workshop* 59. Ministry of Supply and Services, Canada.
- Hedrick, R. 2009. Generation of hourly design-day weather data (RP-1363). ASHRAE Research Project, *Final Report*.
- Huang, Y.J., F.X. Su, D.H. Seo, and M. Krarti. 2014. Development of ASHRAE IWEC2 weather files from the Integrated Surface Hourly (ISH) data base of historical weather data for 3,012 international locations. *ASHRAE Transactions* 120(1):340–355.
- Hubbard, K., K. Kunkel, A. DeGaetano, and K. Redmond. 2004. Sources of uncertainty in the calculation of the design weather conditions in the *ASHRAE Handbook of Fundamentals* (RP-1171). ASHRAE Research Project, *Final Report*.
- Inness, A., et al. 2013. The MACC reanalysis: An 8 yr data set of atmospheric composition. *Atmospheric Chemistry and Physics* 13(8):4073–4109. www.atmos-chem-phys.net/13/4073/2013/acp-13-4073-2013-discussion.html.
- IPCC. 2015. *AR5 Synthesis Report: Climate Change 2014*. International Panel on Climate Change, World Meteorological Organization, Geneva. www.ipcc.ch/report/ar5/syr/.
- Iqbal, M. 1983. *An introduction to solar radiation*. Academic Press, Toronto.
- ISO. 2007. Hygrothermal performance of buildings—Calculation and presentation of climatic data—Part 6: Accumulated temperature differences (degree days). *Standard 15927-6*. International Organization for Standardization, Geneva.
- Kasten, F., and T. Young. 1989. Revised optical air mass tables and approximation formula. *Applied Optics* 28:4735–4738.
- Lamming, S.D., and J.R. Salmon. 1996. Wind data for design of smoke control systems (RP-816). ASHRAE Research Project, *Final Report*.
- Lamming, S.D., and J.R. Salmon. 1998. Wind data for design of smoke control systems. *ASHRAE Transactions* 104(1A):742–751.
- Livezey, R.E., K.Y. Vinnikov, M.M. Timofeyeva, R. Tinker, and H.M. Van Den Dool. 2007. Estimation and extrapolation of climate normals and climatic trends. *Journal of Applied Meteorology and Climatology* 46:1759–1776.
- Lott, J.N. 2004. The quality control of the integrated surface hourly database. 84th American Meteorological Society Annual Meeting, Seattle, WA. ams.confex.com/ams/pdfpapers/71929.pdf.
- Lowery, M.D., and J.E. Nash. 1970. A comparison of methods of fitting the double exponential distribution. *Journal of Hydrology* 10(3):259–275.
- Molod, A., L. Takacs, M. Suarez, and J. Bacmeister. 2015. Development of the GEOS-5 atmospheric general circulation model: Evolution from MERRA to MERRA2. *Geoscientific Model Development* 8:1339–1356.
- NCDC. 1996. *International station meteorological climate summary (ISMCS)*. National Climatic Data Center, Asheville, NC.
- NCDC. 1999. *Engineering weather data*. National Climatic Data Center, Asheville, NC.
- Oke, T.R. 1987. *Boundary layer climates*, 2nd ed. Methuen, London.
- Perez, R., P. Ineichen, R. Seals, J. Michalsky, and R. Stewart. 1990. Modeling daylight availability and irradiance components from direct and global irradiance. *Solar Energy* 44(5):271–289.
- Qiu, X., M. Roth, H. Corbett-Hains, and F. Yang. 2016. Mesoscale climate modeling procedure development and performance evaluation (RP-1561). *ASHRAE Transactions* 122(2).
- Roth, M. 2016. Updating climatic design data in the 2017 *ASHRAE Handbook—Fundamentals*. ASHRAE Research Project RP-1699, *Final Report*.
- Roth, M. 2019. Evaluation of climate reanalysis data for use in *ASHRAE Applications*. ASHRAE Research Project RP-1745, *Final Report*.
- Roth, M. 2021. Updating climatic design information for the 2021 *ASHRAE Handbook*, *Standard 169*, and the *Handbook of Smoke Control Engineering*. ASHRAE Research Project RP-1847, *Final Report*.
- Saha, S., S. Moorthi, X. Wu, J. Wang, S. Nadiga, P. Tripp, D. Behringer, et al. 2014. The NCEP climate forecast system version 2. *Journal of Climate* 27:2185–2208.
- Schoenau, G.J., and R.A. Kehrig. 1990. A method for calculating degree-days to any base temperature. *Energy and Buildings* 14:299–302.
- Sengupta, M., Y. Xie, A. Lopez, A. Habte, G. MacLaurin, and J. Shelby. 2018. The National Solar Radiation Data Base (NSRDB). *Renewable and Sustainable Energy Reviews* 89:51–60.
- Smith, A., N. Lott, and R. Vose. 2011. The integrated surface database: Recent developments and partnerships. *Bulletin of the American Meteorological Society* 92(6):704.
- Thevenard, D. 2009. Updating the ASHRAE climatic data for design and standards (RP-1453). ASHRAE Research Project, *Final Report*.
- Thevenard, D., and C. Gueymard. 2013. Updating climatic design data in Chapter 14 of the 2013 *Handbook of Fundamentals* (RP-1613). ASHRAE Research Project RP-1613, *Final Report*.
- Thevenard, D., and K. Haddad. 2006. Ground reflectivity in the context of building energy simulation. *Energy and Buildings* 38(8):972–980.
- Thevenard, D., J. Lundgren, and R. Humphries. 2005. Updating the climatic design conditions in the *ASHRAE Handbook of Fundamentals* (RP-1273). ASHRAE Research Project, *Final Report*.
- Turner, W.J.N., M.H. Sherman, and I.S. Walker. 2012. Infiltration as ventilation: Weather-induced dilution. *HVAC&R Research* 18(6):1122–1135.
- Wilcox, S., and W. Marion. 2008. Users manual for TMY3 data sets. *Technical Report NREL/TP-581-43156*. National Renewable Energy Laboratory, Golden, CO. www.nrel.gov/docs/fy08osti/43156.pdf.
- WMO. 2007. The role of climatological normals in a changing climate. *Technical Document 1377*. World Meteorological Organization, Geneva.

BIBLIOGRAPHY

- ASHRAE Weather Data Center. www.ashrae.org/technical-resources/bookstore/weather-data-center.
- ASHRAE. 2020. Weather data for building design standards. ANSI/ASHRAE Standard 169-2020.
- ASHRAE. 2019. Ventilation and acceptable indoor air quality in residential buildings. ANSI/ASHRAE Standard 62.2-2019.
- Klote J.H., J.A. Milke, P.G. Turnbull, A. Kashef, M.J. Ferreira. 2012. *Handbook of smoke control engineering*. ASHRAE.